



**HAL**  
open science

## Investigation of stationary phases performance for eicosanoids profiling in RP-HPLC

Kodjo Nouwade, Sana Tfaili, Pierre Chaminade

► **To cite this version:**

Kodjo Nouwade, Sana Tfaili, Pierre Chaminade. Investigation of stationary phases performance for eicosanoids profiling in RP-HPLC. *Analytical and Bioanalytical Chemistry*, 2021, 413 (26), pp.6551-6569. 10.1007/s00216-021-03618-8 . hal-04529912

**HAL Id: hal-04529912**

**<https://hal.science/hal-04529912>**

Submitted on 2 Apr 2024

**HAL** is a multi-disciplinary open access archive for the deposit and dissemination of scientific research documents, whether they are published or not. The documents may come from teaching and research institutions in France or abroad, or from public or private research centers.

L'archive ouverte pluridisciplinaire **HAL**, est destinée au dépôt et à la diffusion de documents scientifiques de niveau recherche, publiés ou non, émanant des établissements d'enseignement et de recherche français ou étrangers, des laboratoires publics ou privés.

# 1 Investigation of stationary phases performance for eicosanoids 2 profiling in RP-HPLC

3 Authors: Kodjo Nouwade, Sana Tfaili\*, Pierre Chaminade

4 Université Paris-Saclay, Lipides : systèmes analytiques et biologiques, 92296, Châtenay-  
5 Malabry, France.

6 \*Corresponding author: Sana Tfaili

7 Tel: 01 46 83 54 63

8 Mail: [sana.tfaili@universite-paris-saclay.fr](mailto:sana.tfaili@universite-paris-saclay.fr)

9 ORCID [0000-0002-6256-6777](https://orcid.org/0000-0002-6256-6777)

## 10 Abstract

11 Eicosanoids – oxidative derivatives from arachidonic acid – represent biologically active lipid  
12 mediators in inflammatory processes. Different analytical methods treat eicosanoids analysis.  
13 Among which reverse phase liquid chromatography figures as the appropriate method for  
14 eicosanoids profiling. RP-HPLC for eicosanoids analysis is often conducted on C18 columns.  
15 Some studies focused on profiling one family of eicosanoids, other considered all eicosanoids  
16 families. In both cases, co-elution remained a major issue and detection in mass spectrometry  
17 partially resolves this problem. In fact, the mass transitions used to monitor eicosanoids species  
18 are not specific enough and many isobars can be listed. For this, optimizing the RP-HPLC  
19 separation remains important. Based on the parameter  $F_s$  – deriving from hydrophobic-  
20 subtraction model – and radar plots, we chose columns with different selectivity. The  
21 hydrophobic-subtraction model guided our interpretation of molecular interactions between  
22 eicosanoids and stationary phases. We founded our approach for selectivity optimization on peak  
23 capacity per minute and time needed values. Herein, we screened seven stationary phases and  
24 evaluated their chromatographic performances in RP-HPLC. Stationary phases presented  
25 different chemistry, type of silica, length, and particles size. Superficially porous particles  
26 columns registered better chromatographic profiles than classical stationary phases; and columns  
27 with embedded polar group did not serve our purpose. The stationary phase Accucore C30 –  
28 even being the least retentive – revealed the best selectivity, efficiency and recorded the shorter  
29 duration for eicosanoids analysis.

30  
31 **Keywords:** Accucore C30, eicosanoids, hydrophobic-subtraction model, selectivity, peak  
32 capacity per minute, time needed.

## 33 **1 Introduction**

34 Eicosanoids are highly active biological lipids. They are involved in many pharmacological and  
35 physiopathological processes. In mammals, eicosanoids mediate a wide array of biological  
36 processes and diseases such as atherosclerosis, diabetes, Alzheimer, cancer, etc. [1]. Literature  
37 mentions three eicosanoids precursors, which are Arachidonic Acid (AA), Eicosapentaenoic  
38 Acid (EPA) and Di-Homo Gamma Linolenic Acid (DGLA). These precursors are implicated in  
39 the synthesis of three subfamilies of eicosanoids as following: prostaglandins, thromboxanes and  
40 leukotrienes [2]. Pathways giving rise to eicosanoids are involved in inflammatory processes.  
41 For decades, non-steroidal anti-inflammatory drugs such as acetylsalicylic acid and ibuprofen  
42 have been used to inhibit prostanoids formation in order to treat inflammatory diseases [3].  
43 Eicosanoids occur at low concentrations – picomolar and nanomolar – in biological matrices and  
44 are highly active molecules [4]. They present a limited stability since they are lipid mediators in  
45 response to specific biological processes. Eicosanoids play opposite or redundant roles, most  
46 often leading to a targeted response, which is the result of a whole cascade of cellular signaling.  
47 The global balance between different species of polyunsaturated fatty acids (PUFA) seems to  
48 modulate various biological processes. Due to their inconstant presence, their low quantity in  
49 biological fluids, and the multiplicity of eicosanoids species in different subfamilies, their  
50 analysis remains an analytical challenge.

51 Among several conducted approaches, literature describes the immunoenzymatic assays for  
52 eicosanoids quantification [5]. Immunoenzymatic assays are limited in the availability,  
53 specificity and selectivity of antibodies [4, 6–8]. In addition, oxidation occurs in biological  
54 processes and complicates eicosanoids quantification. VanRollins and VanderNoot used  
55 capillary electrophoresis to quantify EETs/DHETs regioisomers and stereoisomers and they  
56 underlined selectivity problems between structurally close species [9]. Gas chromatography  
57 coupled to tandem mass spectrometry (GC-MS/MS) was also extensively performed [4] and  
58 allowed, after a derivatization step, to reach a detection limit at the pg/mL level. Because of the  
59 three labile functions of eicosanoids and the difficulty to use the same derivatization agent [10],  
60 these previously described techniques are nowadays forsaken in favor of liquid chromatography.  
61 High performance liquid chromatography (HPLC) methods coupled with tandem mass  
62 spectrometry permitted to identify and quantify eicosanoids with considerable time saving, better  
63 sensitivity, specificity and above all covering a wide range of mediators. Despite the advances in  
64 liquid chromatography, selectivity problems persist between structurally close eicosanoids such  
65 as mono species of prostaglandins, hydroxyeicosatetraenoic acid (HETE). Eicosanoid studies in  
66 RP-HPLC treated quantitative or qualitative profiling of one subfamily of eicosanoids (for

67 example prostanoids); regioisomers separation optimizing (for EET and DiHETE); and sample  
68 preparation [11, 12]. To shorten analysis time, Ubhayasekera, *et al.* proposed a novel approach  
69 for eicosanoids analysis in SFC-MS/MS on five AA metabolites [13]. However, Berkecz, *et al.*  
70 concluded in a comparison study that UHPLC/MS offers a better separation and higher  
71 sensitivity compared to UHPSFC/MS for oxylipins analysis in human plasma [14]. Detection of  
72 eicosanoids is frequently carried out in mass spectrometry [1, 15]. Rarely, other detectors are  
73 encountered such as fluorescence [16] and UV through a derivatization with a reagent which  
74 absorbs light at a higher wavelength [17]. Mass transitions used to monitor eicosanoids species  
75 are not specific enough and many isobars can be listed. Besides isobars, ion suppression  
76 phenomena occurs also and complicates quantification. Hence optimizing the RP-HPLC  
77 dimension remains important. Herein, we focused on stationary phase's selection to optimize  
78 chromatographic profiling of eicosanoids. In order to increase chromatographic efficiency and  
79 selectivity, the development of stationary phases experienced a great rise and a wide range of  
80 stationary phases is currently available. Among which C18 columns are the most used for  
81 eicosanoids analysis according to literature, and columns with embedded polar groups (EPG)  
82 [18] and partially porous particles [2] performed the best chromatographic profiles. Faced by this  
83 diversity, the choice of the appropriate stationary phase is a key step of chromatographic method  
84 development [19].

85 To develop our eicosanoids separation we carefully selected a restricted set of stationary phases  
86 from which different retention properties were expected, we also selected specific species of  
87 eicosanoids involved in atherosclerosis. Eicosanoids mediators have opposite and redundant  
88 properties. It is the overall balance between various oxygenated species which modulates  
89 inflammatory processes. For understanding their roles as potential biomarkers for disease  
90 diagnosis or prognosis, it is important to carefully choose the species for the method reliability.  
91 Thus, eicosanoids which were chosen to elucidate disease pathways must be related to  
92 metabolomics scheme.

93 In order to explain the retention mechanism in RP-HPLC, numerous theories have been  
94 developed. Among them, the solvophobic theory describes the phenomenon responsible for  
95 solute retention as a reversible association process between the hydrocarbonaceous ligand  
96 anchored to the surface and the solute molecule [20]. However, solvophobic theory does not  
97 allow to elucidate the total interactions involved in RP-HPLC separation. Other models tended to  
98 explain retention in RP-HPLC among the hydrophobic subtraction model [21]. Herein, seven  
99 RP-HPLC stationary phases were selected on the basis of predicted selectivity according to  
100 hydrophobic-subtraction model and radar plots illustrations. Chromatographic performances

101 such as selectivity and other descriptors including time needed and peak capacity per minute  
102 (both explained in the theory / calculation section) were also evaluated.

103  
104 **2 Theory / Calculation**  
105 We referred to HPLC database [22] and picked up predicted values to characterize the selectivity  
106 of the seven stationary phases. The parameter  $F_s$  – deriving from hydrophobic-subtraction model  
107 – permitted to choose columns with different selectivity. Time needed and peak capacity per  
108 minute guided selectivity optimization.

### 109 **2.1 Peak capacity per minute**

110 Resolution describes only the separation performance of two consecutive peaks and does not  
111 allow describing at fair value the performance of the whole separation. Horvath and Lipsky  
112 described peak capacity in 1967 as the most common criterion to measure chromatographic  
113 separation capacity [23].

114 In 2005, Neue defined peak capacity  $P_c$  as the number of peaks that can be separated within a  
115 retention window ranking from  $t_1$  to  $t_2$  [24]. The peak width represents four times the value of  
116 the standard deviation of a peak ( $4\sigma$ ). Peak capacity can be expressed in the following integral  
117 form:

$$118$$
$$119 \mathbf{P_c} = \mathbf{1} + \int_{t_0}^{t_r} \frac{1}{4\sigma} dt$$

120 **(1)**

121 Where  $t_r$  is the retention time of the solute and  $t_0$  is the hold-up time, or unretained time [24].

122  
123 Other equations derive from equation (1) and consider variables which influence  
124 chromatographic behavior whether in isocratic or gradient elution modes. Numerous variables  
125 such as retention mechanisms, structure of molecules and stationary phases influence the width  
126 of the peak. Thereby, all factors – which contribute to spread or compress peak – should be  
127 considered to determine the quality of separation in gradient elution. Assuming that the peaks  
128 width in the chromatogram is similar, the integration and simplification of equation (1) yield to  
129 [24]:

$$130$$
$$131 \mathbf{P_c} = \mathbf{1} + \frac{t_g}{\left(\frac{1}{n}\right) \sum_1^n \omega}$$

132 **(2)**

133 where  $t_g$  is the gradient run time,  $n$  is the number of selected peaks and  $w$  the width of each peak  
134 – selected for the calculation – in the chromatogram.

135 For the calculation, selected peaks need to be representative of the distribution of the peak width  
136 throughout the chromatogram. Neue [24] simply considers peak capacity as the gradient run time  
137 divided by the average peak width.

138 In order to normalize different gradient elution modes between linear gradient and optimized  
139 gradient for each stationary phase, we defined an additional parameter of peak capacity per  
140 minute. This parameter allowed us to normalize data and enabled a better comparison between  
141 stationary phases. Thus, peak capacity per minute is the measure of the number of peaks that can  
142 be contained in one-minute elution time window.

143

$$144 \quad P_c / \text{min} = \frac{P_c}{t_g}$$

145 (3)

146

147 By combining equation (2) and (3), we deduced equation (4) as following:

148

$$149 \quad P_c / \text{min} = \frac{1 + \frac{t_g}{\left(\frac{1}{n}\right) \sum_1^n \omega}}{t_g} = \frac{1}{t_g} + \frac{1}{\left(\frac{1}{n}\right) \sum_1^n \omega}$$

150 (4)

## 151 2.2 Time needed

152 Besides peak capacity, time needed is another important criterion to consider in chromatography.

153 To optimize selectivity in high-pressure liquid chromatography, P.J. Schoenmakers defined the  
154 time needed ( $[t_{ne}]_{f,d}$ ) as the minimal time required for separation of complex mixture with a  
155 minimal selectivity [25]. The minimum time required ( $[t_{ne}]_{f,d}$ ) depends of the retention factor and  
156 the minimum selectivity as follows:

157

$$158 \quad [t_{ne}]_{f,d} = \frac{1 + k_{\omega}}{S_{\min}^2}$$

159 (5)

160

161 Where  $f$  = constant flow rate;  $d$  = constant particle diameter

162  $k_{\omega}$  = retention factor of the last peak in the chromatogram,

163 and  $S_{\min}$  = selectivity of the critical pair of peaks within the chromatogram.

164

## 165 **3 Experimental**

### 166 **3.1 Chemicals and columns**

#### 167 **3.1.1 Chemicals**

168 Water and isopropanol HPLC-MS grade were purchased respectively from VWR and Biosolve.

169 Acetonitrile and methanol both HPLC grade from Sigma-Aldrich were used for HPLC analysis.

170 Molecules including eicosanoids, related oxidized and two eicosanoids precursors were

171 purchased from Cayman chemicals (Ann Arbor, MI, USA). The study includes the following

172 twenty six molecules: 6-keto PGF1 $\alpha$  , PGI2 , TXB1, TXB2, PGE3 , PGF2 $\alpha$ , PGE2, PGD2,

173 LXA4, ( $\pm$ )14(15)-DiHETE , LTB4 , LTD4, ( $\pm$ )5(6)-DiHETE, ( $\pm$ )5-HEPE, ( $\pm$ )20-HDHA, ( $\pm$ )9-

174 HODE, ( $\pm$ )15-HETE, ( $\pm$ )12-HETE , ( $\pm$ )11-HETE , ( $\pm$ )8-HETE, ( $\pm$ )5-HETE, ( $\pm$ )8(9)-EET,

175 Carbocyclic Thromboxane A2 or CTA2, ( $\pm$ )14(15)-EET, Eicosapentaenoic Acid or EPA,

176 Arachidonic Acid or AA. It is important to note that two mixtures were preconceived by Cayman

177 Chemistry: Primary Eicosanoid HPLC Mixture (6-keto PGF1 $\alpha$ ; TXB1; PGF2 $\alpha$ ; PGE2; PGD2 )

178 and ( $\pm$ ) HETE mixture (( $\pm$ )15-HETE; ( $\pm$ )12-HETE ; ( $\pm$ )11-HETE ; ( $\pm$ )8-HETE; ( $\pm$ )5-HETE).

179 Eicosanoids' structures are summarized in Electronic Supplementary Material 1, ESM\_1, table

180 1.

#### 181 **3.1.2 Stationary phases**

182 Various column chemistries (C18, C30, and Polar-RP) were tested as listed in table 1. Accucore

183 C30 and Hypersil Gold C18 were purchased from ThermoFisher Scientific (Langerwehe,

184 Germany). ThermoFisher Scientific lent us Accucore C18 and Accucore Polar Premium

185 columns. Cortecs Shield RP18 was kindly provided by its manufacturer Waters ( Milford, PA,

186 USA). Zorbax Bonus RP was purchased from Agilent technologies (Little Fall, NJ, USA) and

187 Nucleodur C18 Isis was purchased from Machery Nagel (Düren, Germany). The main

188 characteristics of the silica particles and the chemistry of stationary phases are detailed in Table

189 1.

### 190 **3.2 Sample preparation**

191 All standards were evaporated under a stream of nitrogen and solubilized in methanol of HPLC

192 grade to have a concentration of 50  $\mu$ g/mL, then stored at -80°C. In addition to the preconceived

193 mixture (HPLC mixture and ( $\pm$ ) HETE mixture), another mixture was prepared at a  
194 concentration of 50  $\mu\text{g/mL}$  and gathered eicosanoid standards and eicosanoid precursors (AA  
195 and EPA).

### 196 **3.3 Chromatographic conditions**

197 Samples were analyzed by an UHPLC system (ThermoFisher Scientific Ultimate 3000) coupled  
198 with a Charged Aerosol Detector (Corona-CAD<sup>®</sup>) equipped with a nitrogen generator. Corona-  
199 CAD<sup>®</sup> parameters were set as follow: gas pressure: 35 Psi; total flow = 1.53; flow ratio = 0.39;  
200 electrometer heater = 35°C; corona voltage = 2.34 kV; Icor = 1,00Ua; IonT = 20,4 V; range =  
201 100 pA. To compare the columns chromatographic performances for eicosanoids separation in  
202 RP-HPLC, two different approaches were investigated. First, we evaluated a linear gradient from  
203 0% to 95% solvent B in 26 min (see Electronic Supplementary Material 2, ESM\_2 table1).  
204 Secondly, the system solvent and gradient was optimized to ensure the best separation for each  
205 column. All eluents such as mobile phase A and mobile phase B were degassed prior to their  
206 usage. In linear gradient, phase A consisted in Water/Acetonitrile/Formic acid (69.96:30:0.04,  
207 v/v/v) and phase B in Acetonitrile/ Formic Acid (99.96:0.04, v/v). All methods were developed  
208 with chromatographic conditions as shown in **see Electronic Supplementary Material,**  
209 **ESM\_2, table 3**, including stationary phases and solvents composition. Temperature was set at  
210 25°C and injection volume was set to 1  $\mu\text{L}$  with a flow rate of 0.5 mL/min. Temperature and pH  
211 were also optimized.



**Table 1** The characteristics of the seven columns used for the development of eicosanoids separation by RP-HPLC

<i>Supplier</i>	<i>ThermoFisher Scientific</i>	<i>ThermoFisher Scientific</i>	<i>ThermoFisher Scientific</i>	<i>Waters</i>	<i>Agilent</i>	<i>Machery Nagel</i>	<i>ThermoFisher Scientific</i>
	<i>Partially porous silica</i>				<i>Fully porous silica</i>		
<b>Columns</b>	Accucore™ C30	Accucore™ C18	Accucore™ C18 Polar	Cortecs Shield RP 18	Zorbax BONUS-RP	Nucleodur C18 Isis	Hypersil Gold C18
<b>Packing Material</b>	Solid core particle. C30	Solid core particle. C18	Solid core particle. C18. Embedded amide group	Solid core particle. C18. Embedded carbamate group	Bonus-RP with an embedded amide linkage in the C14-alkyl chain	C18. Ultrapure Silica	C18. Ultrapure Silica
<b>Pore size (Å)</b>	150	80	150	90	80	110	175
<b>Particule size (µm)</b>	2.6	2.6	2.6	1.6	3.5	1.8	3
<b>Inner diameter (mm)</b>	2.1	2.1	2.1	2.1	2.1	2.0	2.1
<b>Length (mm)</b>	100	100	100	100	50	50	50
<b>Surface area (m<sup>2</sup>/g)</b>	90	130	90	100	180	340	220
<b>Carbone load (%)</b>	5	9	9	6.4	9.5	20	11
<b>End capped</b>	Yes	Yes	Yes	Yes	Triple	Yes	Yes

**Table 2** The predicted values in hydrophobic-subtraction model to characterize stationary phases' selectivity [22]

<b>Name</b>	<b>Silica type</b>	<b>H</b>	<b>S*</b>	<b>A</b>	<b>B</b>	<b>C (pH 2.8)</b>	<b>C (pH 7.0)</b>
<b>Accucore C30</b>	B	0.978	-0.02	-0.143	-0.002	0.321	0.462
<b>Accucore C18</b>	B	1.09	0.054	0.055	-0.04	0.072	0.095
<b>Accucore Polar Premium</b>	EP	0.871	0.103	-0.567	0.217	-0.207	0.787
<b>Cortecs UPLC Shield RP18</b>	EP	0.869	-0.023	-0.28	0.1	-0.19	0.096
<b>Zorbax Bonus RP</b>	EP	0.65	0.1	-1.04	0.37	-2.97	-1.1
<b>Nucleodur Isis</b>	B	1.02	0.05	-0.07	-0.02	-0.01	0.15
<b>Hypersil GOLD</b>	B	0.88	0	-0.01	0.03	0.16	0.47

## 201 **4 Results and discussion**

202 Eicosanoids analysis needs to combine precise, sensitive and high-throughput methods.  
203 Literature focused on eicosanoids implication in several diseases [1, 3, 26], but it is less  
204 common to find a comparison study resolving selectivity issues between eicosanoids isomers  
205 and isobars. Studies underlined numerous co-elutions [2, 6, 27]. Even if some studies covered  
206 around 170 eicosanoids [2, 6], very few eicosanoids were detected and quantified in human  
207 plasma [2, 13, 18], urine [1, 26], cells supernatants [8, 10, 27] and biological fluids [6].

### 208 **4.1 Targeted eicosanoids species**

209 As our project aims to analyze eicosanoids related to atherosclerosis, we targeted the selection  
210 on 24 different species. Some prostanoids such as PGF<sub>2</sub> $\alpha$  and PGI<sub>2</sub> are vasoactive lipid  
211 mediators while 6-Keto-PGF<sub>1</sub> $\alpha$  is an inactive form of PGI<sub>2</sub>. As, PGI<sub>2</sub> with low half time [28]  
212 is rarely found in biological fluid, we selected 6-Keto PGF<sub>1</sub> $\alpha$  as it might be a marker of the  
213 transient presence of PGI<sub>2</sub>. We have also included HETEs species, LXA<sub>4</sub> and LTB<sub>4</sub>. Indeed,  
214 LXA<sub>4</sub> level differs in function of disease [26] and is known in literature as leukocyte  
215 activation factor and chemotaxis effects. HODE involved in the inflammation resolution in  
216 several disease and EET – Cytochrome P450 product of AA– may potently induce arteriolar  
217 dilatation. In addition, the chosen molecules mimic a complex mixture as some present very  
218 close structures. HETEs species are isomers and isobaric compounds. PGE<sub>2</sub> and PGD<sub>2</sub> are  
219 isomers and isobaric molecules. TXB<sub>1</sub> and TXB<sub>2</sub> share the same structure and differs in one  
220 unsaturation.

### 221 **4.2 Column selection systems in RP-HPLC**

222 To perform eicosanoids separation, we selected columns with different selectivity based on  
223 column selection systems especially Hydrophobic Subtraction Model. Retention mechanism  
224 in RP-HPLC is strongly linked to phenomena at the molecular level. Molecules' structure  
225 induces particular interactions which should be considered before choosing the appropriate  
226 stationary phase. To date, HPLC database [22] report around 751 RP-HPLC columns with  
227 large differences in selectivity. Most of them subtly differ in terms of selectivity, but the  
228 difference is often sufficient to achieve a required separation [19].

229 Several column selection system (CSS) were developed and guided chromatographers in  
230 environmental, biological, pharmaceutical molecules separation, etc. Most of them evaluate  
231 column performance through a ratio between the retention factor of a given molecule and a

232 reference molecule which represents the interaction occurring during chromatographic  
233 process. Based on the ratio of k factor between polar or basic analytes and test compounds,  
234 Engelhardt column selection system (CSS) provided interest information on silanol  
235 accessibility [19]. Drawing inspiration from Engelhardt CSS, Tanaka, *et al.* developed  
236 another system which highlights additional interactions such as hydrogen bonding capacity  
237 and shape selectivity. To select a suitable column with EPG for acid or basic solutes, Layne,  
238 *et al.* CSS has been shown to be advantageous. From 26 to 8 chromatographic probes, Euerby  
239 modified Tanaka CSS and defined the column difference factor (CDF) as the euclidian  
240 distance between a given column and an *a priori* selected reference column [19]. Herein,  
241 Euerby CSS does not serve our purpose as it is difficult to predict which stationary phase can  
242 be chosen as a reference column for eicosanoids isomers and isobars separation. Indeed, the  
243 size, polarity, rigidity, planarity and unsaturation's degree owing to eicosanoids structures  
244 makes difficult the selection of a reference column.

245 A relevant quantitative approach for the prediction of chromatographic retention from the  
246 molecular structure appeared in 1970 and was known as quantitative structure-retention  
247 relationships (QSRRs). In this model introduced by Abraham [21], linear free energy  
248 relationships deriving from solvophobic parameters, are used to predict the chromatographic  
249 retention factors for columns. However, the model do not cover parameters that increase with  
250 retention such as: the shape selectivity, ionic interactions of the cation exchange type and  $\pi$ - $\pi$   
251 complexation phenomena.

252 Hydrophobic subtraction model (HSM) was described by Snyder and co-workers to complete  
253 Abraham model. HSM model makes consensus in the scientific community, as shown in  
254 many applications for column selectivity [19, 21, 29, 30].

255 We have used Hydrophobic Subtraction Model (HSM) and selected 7 columns. In our case,  
256 analyzing eicosanoids without a derivatization step can only be conducted by a universal  
257 detector or Mass spectrometry (MS). All reference compounds in CSS are volatile and cannot  
258 be detected by corona CAD<sup>®</sup>. Consequently, it is less practical to perform the comparison of  
259 column selectivity through most of CSS in the context of eicosanoids.

260 The columns predicted selectivity available on HPLC database [22], was practical to classify  
261 columns. All the interactions during chromatographic process are reported in the database  
262 through different selectivity according to HSM parameters. Indeed, this model was described  
263 to choose a column of very different selectivity and to select replacement columns that will  
264 give the same separation. Overlapping peaks oblige to change or improve column selectivity.  
265 The strength and weakness of HSM model is that the columns are ranked versus 67

266 chromatographic probes which are representative of the different solute-stationary phase  
267 interactions. Other studies reduced the test compounds to 18 and decreased the redundancy of  
268 some solutes in HSM [31]. In our case, eicosanoids exhibit a very few structure variability.  
269 The close structure of eicosanoids steered our approach towards a thoughtful choice of  
270 columns with different selectivity. To take into account the close structure and select columns  
271 with different selectivity, we used  $F_s$  parameter [29]. This permitted to reduce the number of  
272 chosen columns while covering different selectivities. We kept in mind that the Euclidean  
273 distance  $F_s$  expresses the difference in selectivity. One should not forget that for a same  $F_s$ ,  
274 value, the underlying parameters might differ.

### 275 **4.3 The hydrophobic-subtraction model in RP-HPLC**

276 Retention was attributed to solvophobic or hydrophobic interactions [20]. Hydrophobic  
277 interactions and silanol activity contribute to retention but are not enough to define it. Several  
278 models tended to explain retention in RP-HPLC. Snyder, *et al.* described the hydrophobic-  
279 subtraction model – equation 6 – [21] to reflect the contributions from other types of solute-  
280 column interactions.

$$281 \log \alpha \equiv \log \left( \frac{k}{k_{EB}} \right) = \eta' H - \sigma' S^* + \beta' A + \alpha' B + \kappa' C$$

282 (6) (i) (ii) (iii) (iv) (v)

283 The parameters H,  $S^*$ , A, B, C are specific to each column: H (hydrophobicity),  $S^*$  (steric  
284 resistance to insertion of bulky solute molecules into the stationary phase), A (measurement  
285 of hydrogen-bond acidity precisely attributed to non-ionized silanol activity), B (measurement  
286 of hydrogen-bond basicity), C (evaluation of cation exchange interaction between chemical  
287 groups of solute and ionized silanol). Factors  $\eta'$ ,  $\sigma'$ ,  $\beta'$ ,  $\alpha'$ ,  $\kappa'$  are specific to each solute and  
288 vary with the hydrophobicity, the configuration or the spatial geometry of the molecule and  
289 the presence of acid and/or basic groups. Furthermore, it should be noted that the terms (i),  
290 (iii), (iv) and (v) express attractive interactions, which are therefore positive. Only, the term  
291 (ii) relates to a repulsive interaction, which is negative. It is important to note that all these  
292 molecular interactions define the selectivity between molecules during reverse phase  
293 separations.

### 294 4.3.1 Comparison of columns selectivity from HPLC database

295 Based on hydrophobic subtraction model, various column chemistries (C18, C30, and Polar-  
296 RP) were selected as listed in table 1. Among seven columns, three are totally porous particles  
297 columns (Hypersil Gold C18, Nucleodur Isis C18 and Zorbax Fusion RP) and four are  
298 superficially porous particles columns (Accucore C30, Accucore C18, Accucore Polar  
299 Premium, and Cortecs Shield C18). In addition, three columns are polar embedded reversed-  
300 phase columns (Accucore Polar Premium, Cortecs Shield C18 and Zorbax Fusion RP..Table 2  
301 summarizes the predicted values of H, S\*, A, B, C for each stationary phase [22]. We did not  
302 consider the C term at pH=7 since the mobile phase contains formic acid. Polar embedded  
303 reversed-phase columns – Accucore Polar Premium, Cortecs Shield C18 and Zorbax Bonus  
304 RP – show the less hydrophobicity (H values). They also engage less acid hydrogen-bond (A  
305 values) with an acceptor solute and they present the highest basicity. The embedded polar  
306 group (EPG) increases basicity. EPG are amide for Accucore Polar Premium and Zorbax  
307 Bonus RP, and carbamate for Cortecs Shield C18 (the amide basicity is higher than  
308 carbamate) [30]. In addition, both Accucore Polar Premium and Zorbax Bonus RP record the  
309 greatest steric resistance (S\*).

310 The polar embedded reversed-phase columns are the least likely to establish cation exchange  
311 interactions with analytes at acid pH. The limited number of EPG in these columns does not  
312 allow to neutralize utterly the silanol activity at pH 7 (C) as demonstrated by Snyder [21]. By  
313 referring to C values for Accucore C30 (0.321) and Accucore Polar Premium (-0.207) at pH  
314 2.8, we can expect a strong cation exchange interaction for Accucore C30: the low percentage  
315 of grafting in Accucore C30 gives access to a greater amount of free silanol and could explain  
316 this observation.

317 The database [22] provides the parameter  $F_s$  to compare two columns each other.  $F_s$  is defined  
318 as the distance between two columns in the five dimensional plot (H, S\*, A, B and C) [29,  
319 30]. Overall, a  $F_s$  factor  $< 3$  indicates that these two columns are very similar. A  $F_s > 3$   
320 indicates that these two columns are very different [30]. But one should not neglect that  
321 underlying parameters defining  $F_s$  might differ.  $F_s$  derives from hydrophobic-subtraction  
322 model and permits to choose columns with different selectivity. It is calculated according to  
323 the following equation:

$$324 F_s = \sqrt{(12.5(H_1 - H_2))^2 + (100(S_1^* - S_2^*))^2 + (30(A_1 - A_2))^2 + (143(B_1 - B_2))^2 + (83(C_{2.8_1} - C_{2.8_2}))^2}$$

325 (7)

326 Weighing factor varies in function of molecule structure, and depends especially on values of  
327 basicity and cation exchange interactions. Eicosanoids are molecules with polar function and  
328 hydrocarboneous chain. Since eicosanoids are acid carboxylic molecules except the cysteinyl  
329 leukotrienes –which contains amino acids–, we choose the default weighting factor for  $F_s$   
330 calculation: 12.5, 100, 30, 143, 83 are respectively the default weighting factor which  
331 represent the difference in hydrophobicity, steric interactions, hydrogen bond acidity,  
332 hydrogen bond basicity, and charge interactions at pH 2.8.

333 According to  $F_s$  values (Table 3), the stationary phases Accucore C18 and C30 are similar.  
334 Both display equivalent  $F_s$  values with Hypersil Gold ( $F_s=1.15$  and  $F_s=1.49$  respectively). In  
335 addition, Hypersil Gold exhibits a comparable chromatographic behavior with Nucleodur Isis.  
336 Hence, one would expect a similar behavior between Accucore C30 and Nucleodur Isis: this  
337 is not completely true as Accucore C30 and Nucleodur Isis record an  $F_s$  value  $>3$ . Besides,  
338 EPG columns exhibit high  $F_s$  values in comparison with the four previously cited columns  
339 (Accucore C18, Accucore C30, Hypersil Gold and Nucleodur Isis are non-EPG columns).  
340 Among EPG columns, Zorbax Bonus RP – a C14 column with an amide group – is expected  
341 to be significantly different from all other stationary phases. Accucore Polar and Cortecs  
342 Shield are equivalent columns ( $F_s=3.02$ ).

343 Even if  $F_s$  parameter was described to characterize column selectivity, some conclusions  
344 related to this parameter deserves more thorough examination. For example, Hypersil Gold  
345 and Accucore C30 would theoretically provide the same selectivity, same observation could  
346 be underlined between Nucleodur Isis and Accucore C18. For graphical visualization in terms  
347 of selectivity between selected columns, we normalized hydrophobic subtraction model data  
348 for each column to 1. Fig.1 illustrates the radar plot of normalized data. According to this  
349 plot, Nucleodur Isis and Accucore C18 can be discriminated through factor H and A. Except  
350 cation exchange interaction value and acid hydrogen bond value, Accucore C30 and Hypersil  
351 Gold did not share the same levels of other interactions in hydrophobic subtraction model.  
352 Comparison through both previously presented examples reveal that  $F_s$  parameter alone is not  
353 sufficient to compare columns selectivity. The radar plot displayed for each column alone  
354 (Fig.1) confirms the diversity of predicted selectivity of our selected columns. In addition, the  
355 best eicosanoids profile obtained in RP-HPLC with each column (section 4.6) showed the  
356 diversity behavior of column in terms of ability to separate isomers and isobars of oxylipins.  
357 Among classical columns, Nucleodur C18 Isis – an octadecylsilyl phase with crosslinked  
358 surface modification – enables fast separation of triacylglycerol regioisomers according to

359 Tchaplá, *et al.* [32]. We included stationary phases with EPG in our columns set. The  
 360 secondary polar interactions mediated by the polar embedded reverse-phase could help to  
 361 discriminate eicosanoids isomers especially for prostanoids.

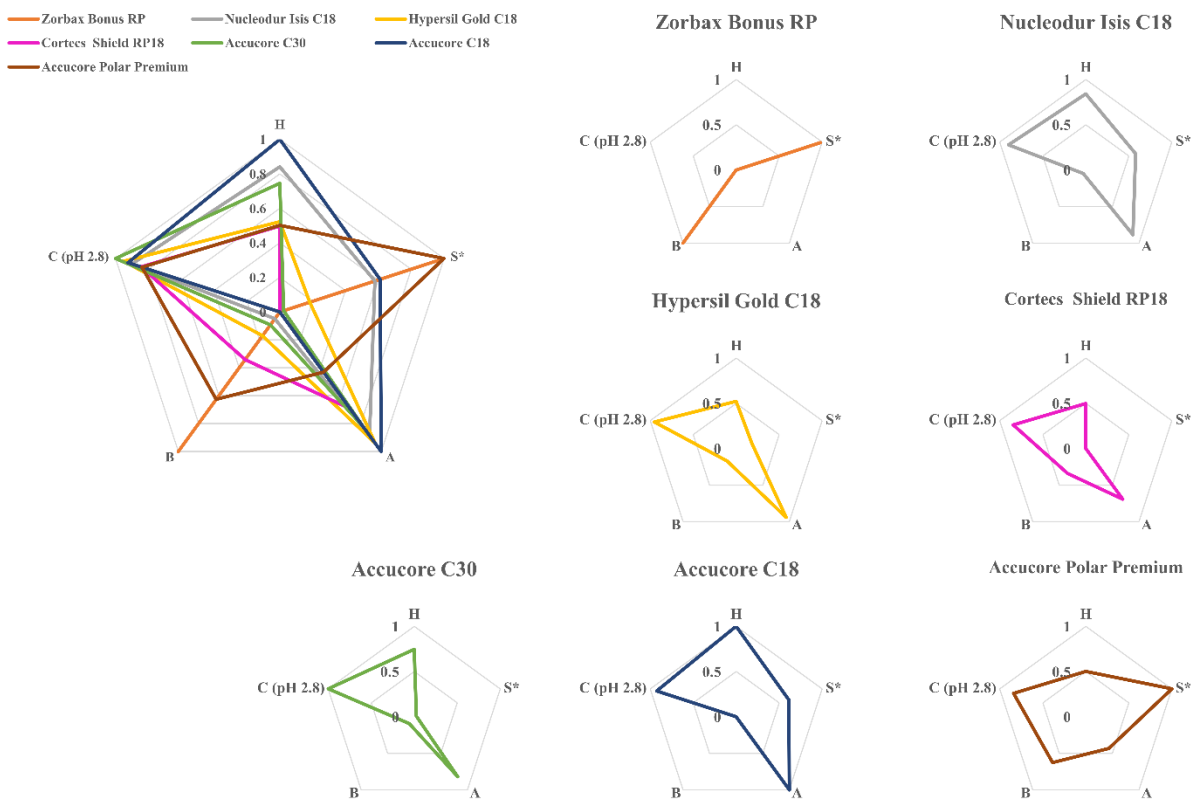


**Fig.1: Radar plot representation of columns comparison based on predicted selectivity according to hydrophobic subtraction model.** H: hydrophobicity, S\*: spatial selectivity, A: hydrogen bond acidity, B: Basicity, and C: the degree of silanol ionization or cation-exchange capacity. Individual values are normalized to the highest value.

**Table 3**  $F_s^*$  parameter calculated for the pairwise comparison of the seven tested columns

<b>Manufacturer</b>	<b>Stationary phases</b>	<i>Accucore</i> C30	<i>Accucore</i> C18	<i>Accucore</i> Polar	<i>Cortecs</i> Shield RP18	<i>Zorbax</i> Bonus RP	<i>Nucleodur Isis</i> C18	<i>Hypersil GOLD</i> C18
<b>Thermo/Hypersil</b>	<i>Accucore C30</i>	0						
<b>Thermo/Hypersil</b>	<i>Accucore C18</i>	<b>3.61</b>	0					
<b>Thermo/Hypersil</b>	<i>Accucore Polar</i>	18.52	14.1	0				
<b>Waters</b>	<i>Cortecs Shield RP18</i>	11.93	6.53	<b>3.02</b>	0			
<b>Agilent</b>	<i>Zorbax Bonus RP</i>	472.82	415.35	322.15	335.66	0		
<b>Macherey Nagel</b>	<i>Nucleodur Isis C18</i>	4.90	<b>0.57</b>	9.61	<b>3.44</b>	389.57	0	
<b>Thermo/Hypersil</b>	<i>Hypersil GOLD C18</i>	<b>1.49</b>	<b>1.15</b>	13.27	6.55	431.58	<b>1.67</b>	0

\* $F_s$  was calculated from hydrophobic-subtraction model values for each column at pH 2.8 (HPLC database) [22] with equation (7). We did not consider the C term at pH=7 since the mobile phase contains formic acid.



## 318 **4.4 Retention factor and efficiency evaluation**

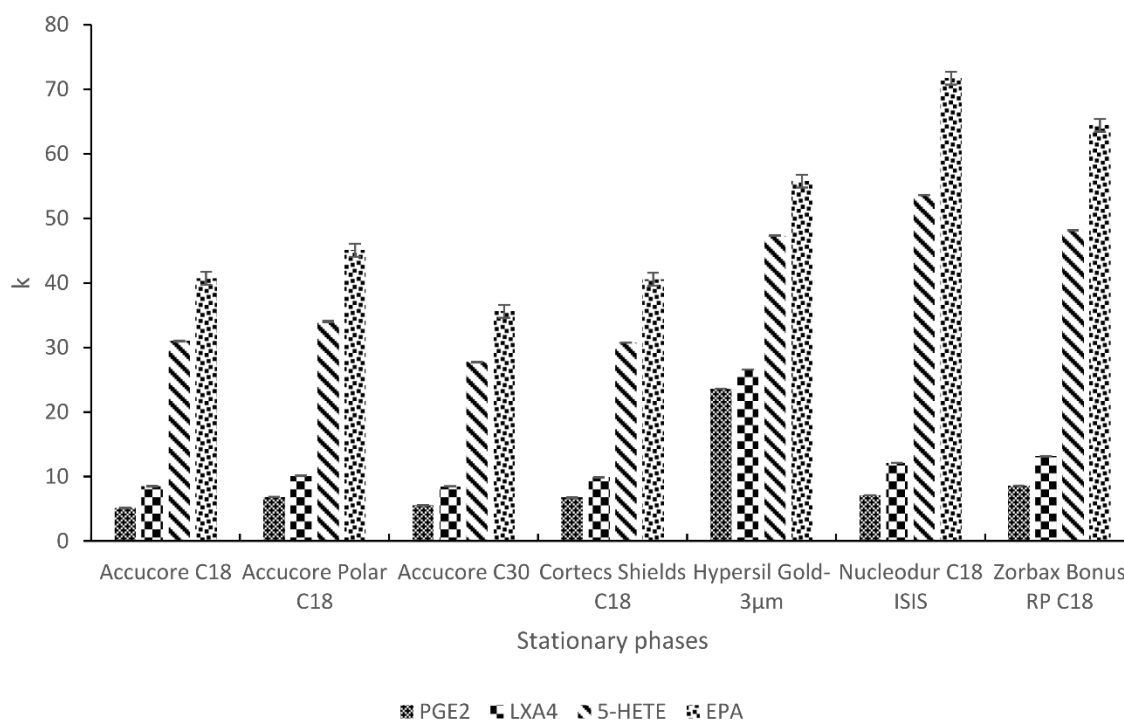
319 We screened the characteristics of 7 RP-HPLC stationary phases (Table 1) which offers  
320 different selectivity (Fig.1) to define which ones are suitable for eicosanoids isomers and  
321 isobars separation. Column assessment was conducted with respect to retention, efficiency  
322 and selectivity.

323

### 324 **4.4.1 Analysis in linear gradient mode**

325 Four representative molecules of the overall eicosanoids profile were chosen for retention  
326 factor calculation. Retention factor ( $k$ ) is calculated for PGE2, LXA4, 5HETE and EPA.  
327 Among the seven columns, Nucleodur C18 Isis phase was the most retentive (Fig.2). The  
328 retention behavior of Nucleodur C18 correlated with a high percentage of carbon grafting  
329 (20%); whereas for other columns it ranges from 5% to 11%. Accucore C30 has the lowest  
330 carbon grafting percentage (5%) and was the least retentive.

331 Despite the substantial difference in carbon load, Hypersil Gold C18 and Accucore C18  
332 (columns without EPG) as well as Cortecs Shield C18 and Accucore C18 Polar (EPG  
333 columns) exhibited comparable retention performance. In addition to the carbon load, which  
334 correlated with retention performance, the EPG mediated secondary polar interactions and  
335 contributed to the retention.



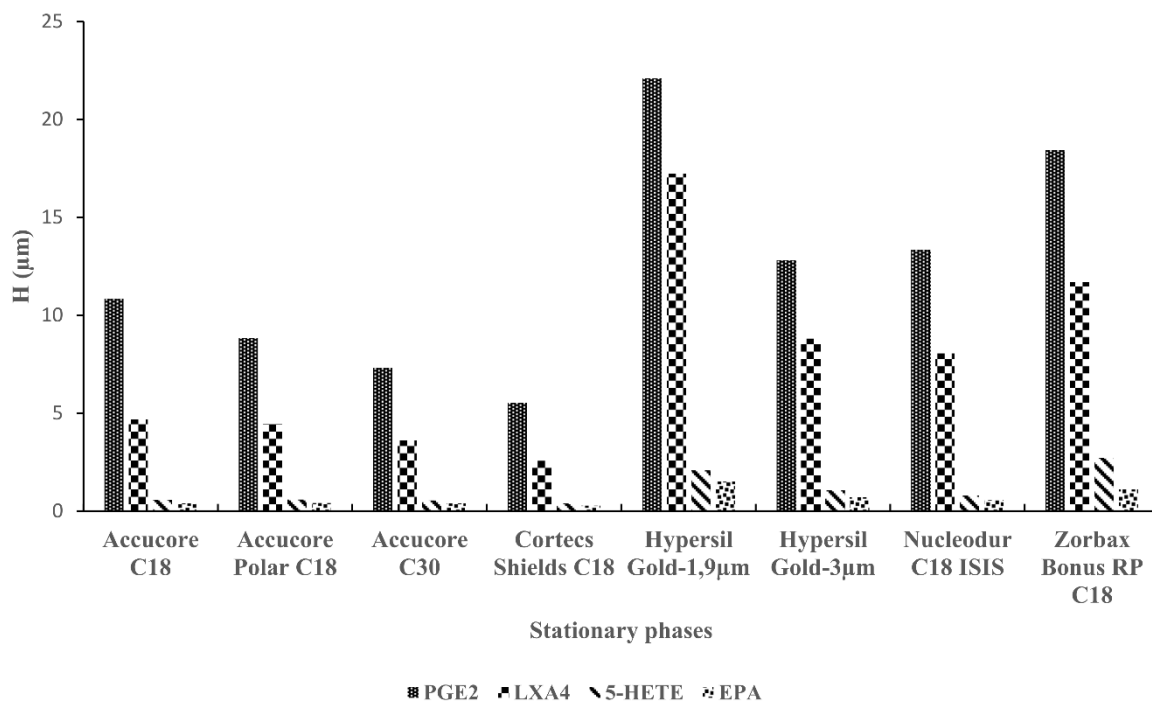
336 **Fig.2: Average of retention factors for four eicosanoids (stationary phases evaluated in linear gradient).** Mobile phase:  
 337 A (Water:ACN, 70:30,v/v) containing 0.04% HCOOH; B(ACN,100,v) containing 0.04%HCOOH ; T = 25°C, average of k  
 338 and standard deviation are calculated on triplicate.

#### 339 4.4.2 Column separation efficiency

340 Among the seven RPLC columns, stationary phases with superficially porous particles  
 341 provide a better efficiency compared to conventional columns (Fig.3). This is expected and is  
 342 already well described in the literature [33]. Accucore C30 and Cortecs shield RP18  
 343 registered similar apparent plate heights and the best efficiency. These columns have an  
 344 efficiency close to the sub-2 µm columns with a much lower pressure drop [33, 34]. The term  
 345 A of Van Deemter equation for superficially porous particles was described merely as the  
 346 homogenous packing and regular shapes of superficially porous particles [35, 36]. Guiochon,  
 347 *et al.* [37, 38] also linked a narrow particle size distribution to high efficiency.

348 Accucore C30 and Accucore Polar present the same pore size (150 Å) but display different  
 349 efficiency. This difference could be attributed to packaging defects causing a lack of  
 350 homogeneity of the particles in the column, especially on the walls [33]. The difference in  
 351 column chemistry of Accucore C30 and Accucore Polar (presence of EPG and length of  
 352 grafted chains) could be another reason for this result. While superficially porous particles  
 353 contributes to produce narrow peaks and allows more peaks to be separated; the nature of  
 354 silica particles did not influence significantly the selectivity between isomers. Indeed, the

355 grafting chemistry is the main factor which contributes to isomers discrimination during  
 356 chromatographic process.

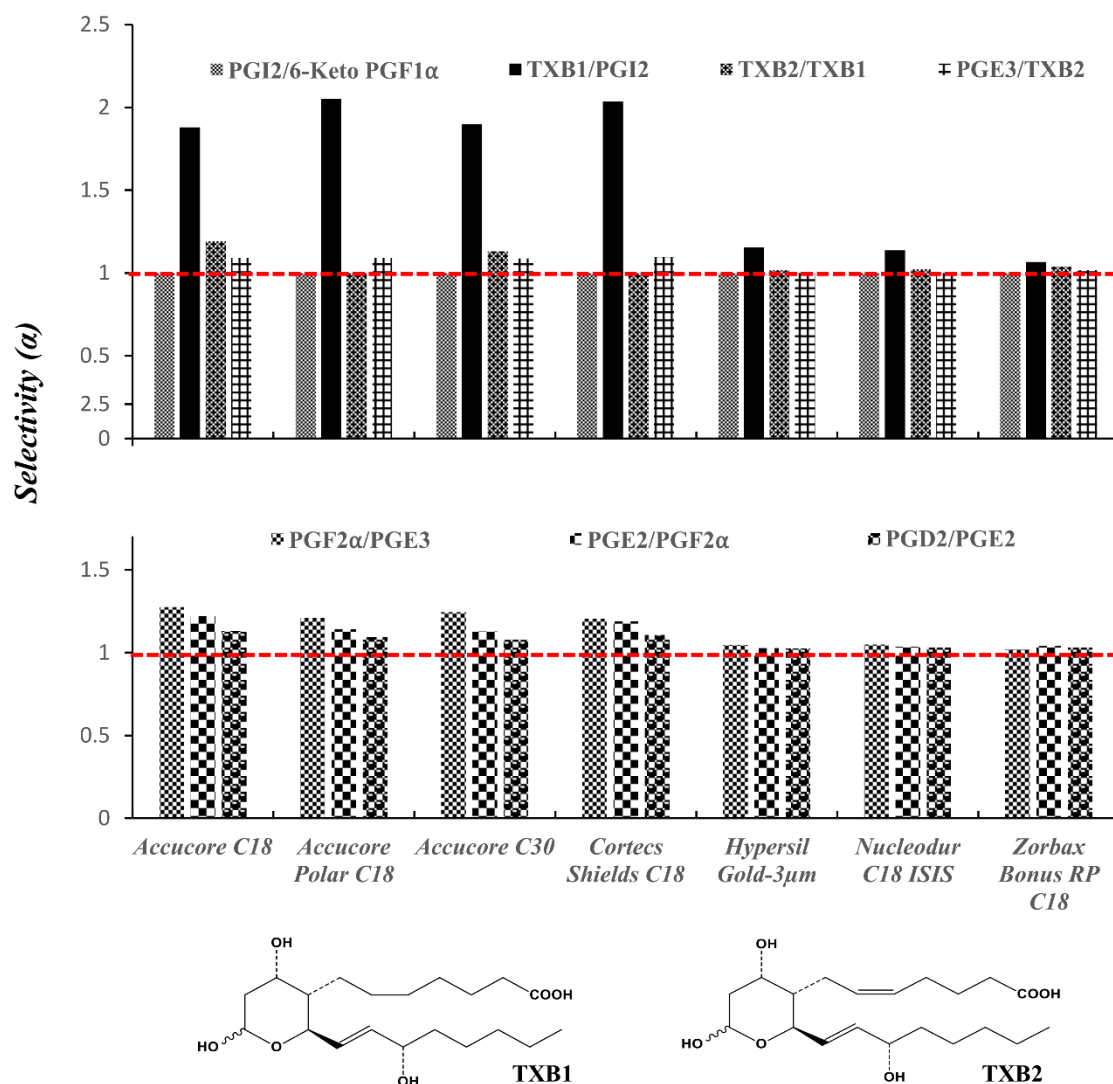


357  
 358 **Fig.3: Efficiency assessment of seven stationary phases in the same gradient linear mode elution.** Efficiency evaluation  
 359 was performed through the parameter H for all columns. Mobile phase: A (Water:ACN, 70:30,v/v) containing 0.04%  
 360 HCOOH; B(Acetonitrile,100,v) containing 0.04% HCOOH ; T = 25°C.

### 361 4.4.3 Differences in selectivity for eicosanoids separation

362 Figure 4 gathers stationary phases into two groups: on one hand, Cortecs Shield and Accucore  
 363 columns (C18, Polar C18 and C30); and on the other hand, Hypersil Gold, Nucleodur Isis and  
 364 Zorbax Bonus RP. Superficially porous particles columns emphasized the best selectivity:  $\alpha$   
 365 value ranged from 1.3 to 2 (Fig.4). Accucore Polar premium and Cortecs Shield C18 – two  
 366 superficially porous particles columns with EPG – exhibited a comparable selectivity and  
 367 confirmed predicted  $F_s$  values previously. The similar chromatographic behavior between the  
 368 latter three stationary phases is striking compared with what we presented above for  $F_s$  values.  
 369 Different chromatographic behavior should have been observed. This could be explained by  
 370 close interactions between prostanoids and stationary phases. A selectivity  $>1$  between  
 371 different species of prostanoids point out a difference in retention factor of molecules. These  
 372 differences in retention are probably due to interactions between solutes and stationary phases  
 373 and  $F_s$  values do not reflect it completely. Columns with EPG underlined two co-elutions  
 374 among prostanoids (6-Keto-PGF1 alpha co-eluted with PGI2 and TXB1 co-eluted with  
 375 TXB2) and other co-elutions in the full RPLC profile of eicosanoids. TXB1 and TXB2 share

376 the similar structures and differ in the number of unsaturation (Fig.4, structures). Unsaturation  
 377 might not be susceptible to polar interactions. Based on the hydrophobic-subtraction model,  
 378 the steric resistance to penetration opposed by grafts of EPG columns might be the main  
 379 cause of the co-elution of TXB1 and TXB2. For our knowledge, literature never reported this  
 380 information for eicosanoids. Thus, this observation confirms the predicted values of S (Table  
 381 2) for EPG columns.

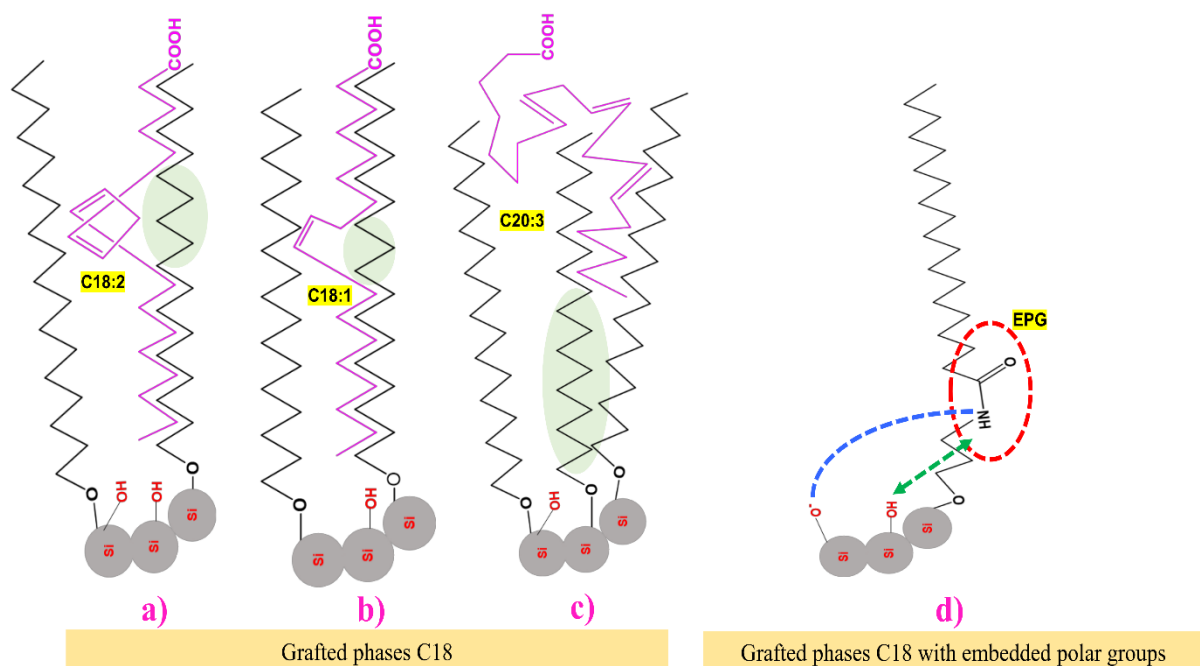


382

383 **Fig.4: Column selectivity evaluated through prostanoids separation.** Phase mobile: A (Water:ACN, 70:30,v/v) containing  
 384 0.04% HCOOH; B(Acetonitrile,100,v) containing 0.04%HCOOH ; T = 25°C.

385 Accucore C30 and Accucore C18 showed one co-elution between 6-keto PGF1 $\alpha$  and PGI2.  
 386 Superficially porous particles columns without EPG registered less co-elutions, come after  
 387 superficially porous particles EPG columns and then classical columns. Steric selectivity and  
 388 functional selectivity explain the columns' performances. Herein, we can underline that the  
 389 functional selectivity characterized EPG columns.

390 To illustrate that the steric selectivity leading to TXB1 and TXB2 co-elution and as  
 391 eicosanoids derive from C20 PUFA, we present in Fig.5 the possible molecular interactions  
 392 between three PUFA (C18:1, C18:2 and C20:3) and reverse phase columns. As shown, each  
 393 unsaturation of PUFA could induce a reduction of the docking area between the solute and the  
 394 stationary phase and reduce retention. In fact, the number and the position of unsaturation  
 395 would imply particular spatial geometry of the molecules while eluting. This geometry  
 396 contributes to the resistance to penetration during the solute-stationary phase interaction. This  
 397 phenomenon makes us wonder if the high grafting percentage would be a limiting factor for  
 398 the penetration of polyunsaturated solutes? The previous question requires another  
 399 investigation to understand the correlation between the polyunsaturated compounds and the  
 400 carbon load in columns. Gilroy, *et al.* reported that S increases with increasing ligand length  
 401 and concentration, and decreases with larger pore diameters [29]. Thus, these findings support  
 402 our hypothesis on a possible relation between steric resistance and high grafting percentage.



403 **Fig.5: Retention mechanism of polyunsaturated fatty acids, steric resistance to penetration and secondary polar**  
 404 **interactions on a C18 phase and a C18 phase with EPG.** a, b and c show the influence of the unsaturations for  
 405 polyunsaturated fatty acids on their retention through reverse phase stationary phase. The green arrows indicate the hydrogen  
 406 bond between a silanol and the carboxyl group of the solute (a donor or acceptor group such as the carbamate of EPG). The  
 407 blue arrows show the ionic interactions (cation exchange) between an ionized silanol and a group of either the stationary  
 408 phase or solute. d is an illustration of a C18 grafted phase with EPG, which is susceptible to various interactions such as  
 409 hydrogen bonding or ion exchange. The molecular interactions between three PUFA (C18:1 for oleic acid, C18:2 for linoleic  
 410 acid, and C20:3 for homo-gamma-linolenic acid) and reverse phase columns during liquid chromatography separations are  
 411 illustrated. As shown, each unsaturation of PUFA induces a reduction of the docking area between the solute and the  
 412 stationary phase, thus implying a reduction in retention. In fact, the number and the position of the unsaturations would imply  
 413 a particular geometry of the molecule resulting in a resistance to penetration during the solute-stationary phase interaction.

414 Indeed, literature highlights the solute penetration for triglycerides in the grafts of reverse  
415 phase columns [39, 40]. Analysis of the retention factors logarithm for triglycerides according  
416 to the number of carbon showed a derivation in slope from a certain number of carbon. The  
417 discontinuity in the linearity of the plot has been explained by Martin, *et al.* [39] as a change  
418 in conformation of the molecules during their penetration into the grafts of the stationary  
419 phases. Due to steric hindrance, the glyceric head is arranged in opposite to the direction of  
420 penetration. NMR and X-Ray spectroscopic studies of triglycerides structural conformations  
421 [41] showed that the two end chains were oriented in the same direction and the middle chain  
422 was in the opposite direction. Therefore, partial penetration occurs due to the steric hindrance  
423 and the presence of double bonds [39]. Consequently, we can deduce that multiple  
424 conformations of eicosanoids could occur during penetration within the grafts. Altogether,  
425 efficient separation of eicosanoids regioisomers or stereoisomers could be improved with a  
426 sufficient steric recognition by the grafts. Other interactions including hydrogen or ion  
427 exchange occur during a chromatographic separation (Fig.5.d). It concerns EPG columns  
428 especially. The outstanding selectivity of EPG columns as described [18] would come from  
429 the specific interactions such as hydrogen bond and ion exchange compared to columns  
430 without EPG. These results accord with the literature [42, 43].

## 431 **4.5 Peak capacity and time needed**

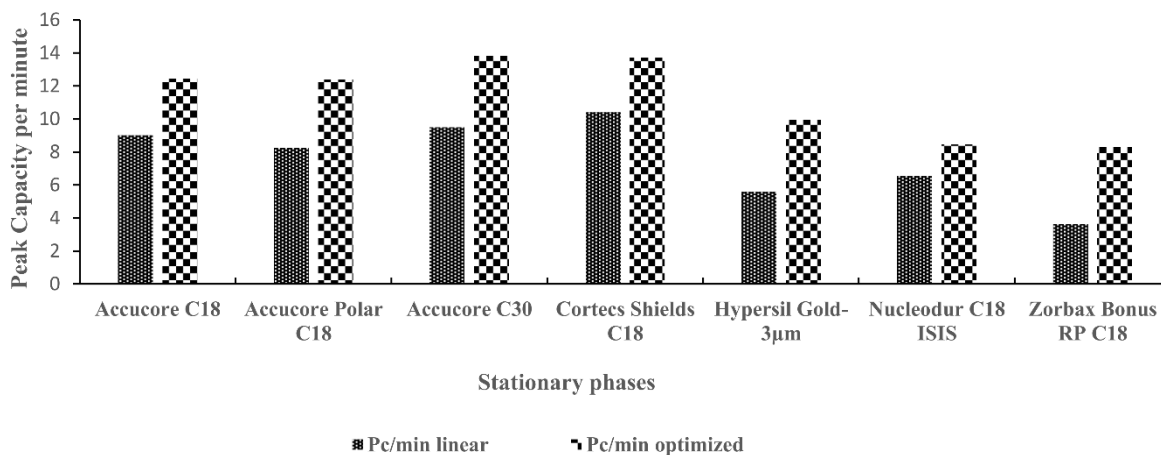
432 Two other chromatographic separation criteria – time needed and peak capacity – were  
433 applied to eicosanoids analysis and helped to discriminate our columns. Time needed and  
434 peak capacity descriptors permitted to evaluate selectivity and helped to measure the  
435 separation over the entire chromatographic domain. Peak capacity per minute illustrates the  
436 number of peaks that can be separated within a retention window and is a common criterion to  
437 measure chromatographic separation capacity. Indeed, time needed is a criterion to optimize  
438 selectivity.

439

### 440 **4.5.1 Peak capacity**

441 Peak capacity calculation is appropriate if the peak width is representative of all peaks in the  
442 chromatogram. All peak widths in our chromatographic profile were similar except 6-Keto  
443 PGF1 $\alpha$ .

444 Results in Fig.6 exhibit a greatest peak capacity for optimized gradient compared to linear  
 445 gradient. Accucore C30 and Cortecs Shield C18 revealed the highest peak capacity. This is  
 446 expected as superficially porous particles properties improve the peak capacity.

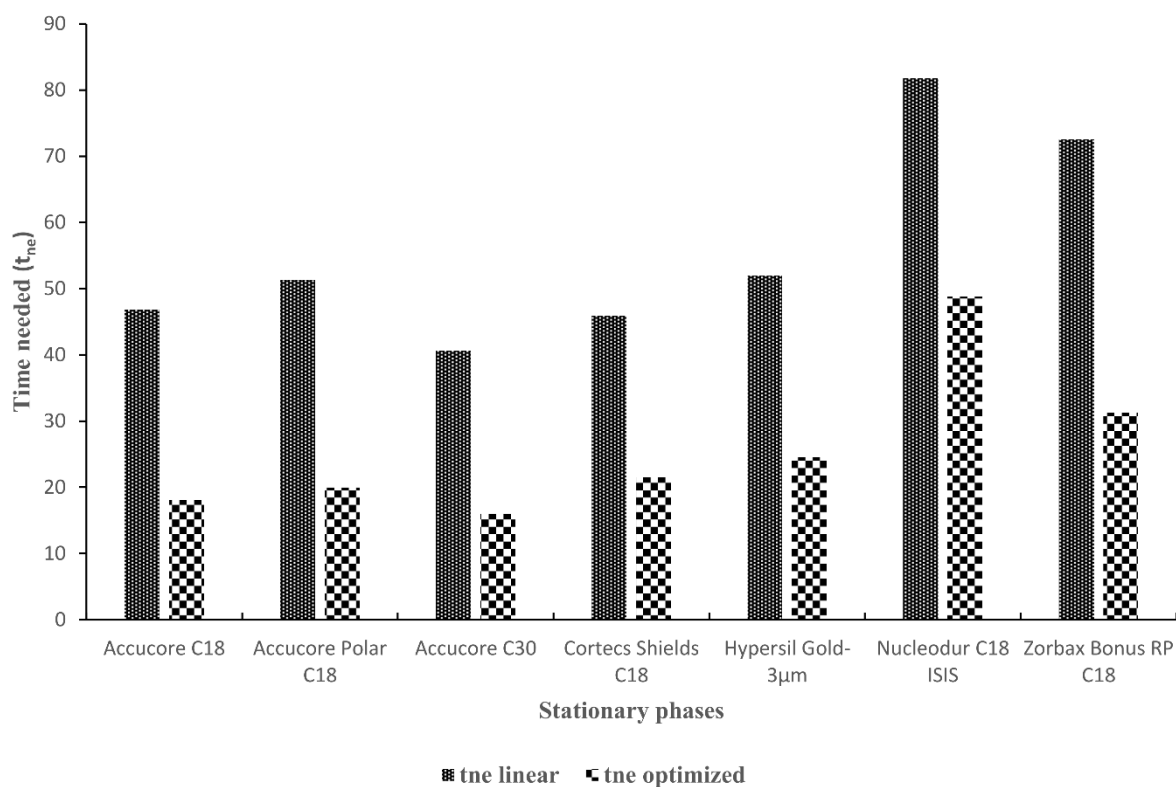


447  
 448 **Fig.6: Peak capacity per minute for the seven stationary phases.** Linear gradient (mobile phase: A (Water:ACN,  
 449 70:30,v/v) containing 0.04% HCOOH; B(Acetonitrile,100,v) containing 0.04%HCOOH ; T = 25°C ; V injec = 1µL ; Flow  
 450 rate = 0.5 mL/min). For more details on optimized gradient conditions, see **Electronic Supplementary Material, ESM\_2**  
 451 **table 2 and table 3.**

#### 452 4.5.2 The time needed ( $t_{ne}$ )

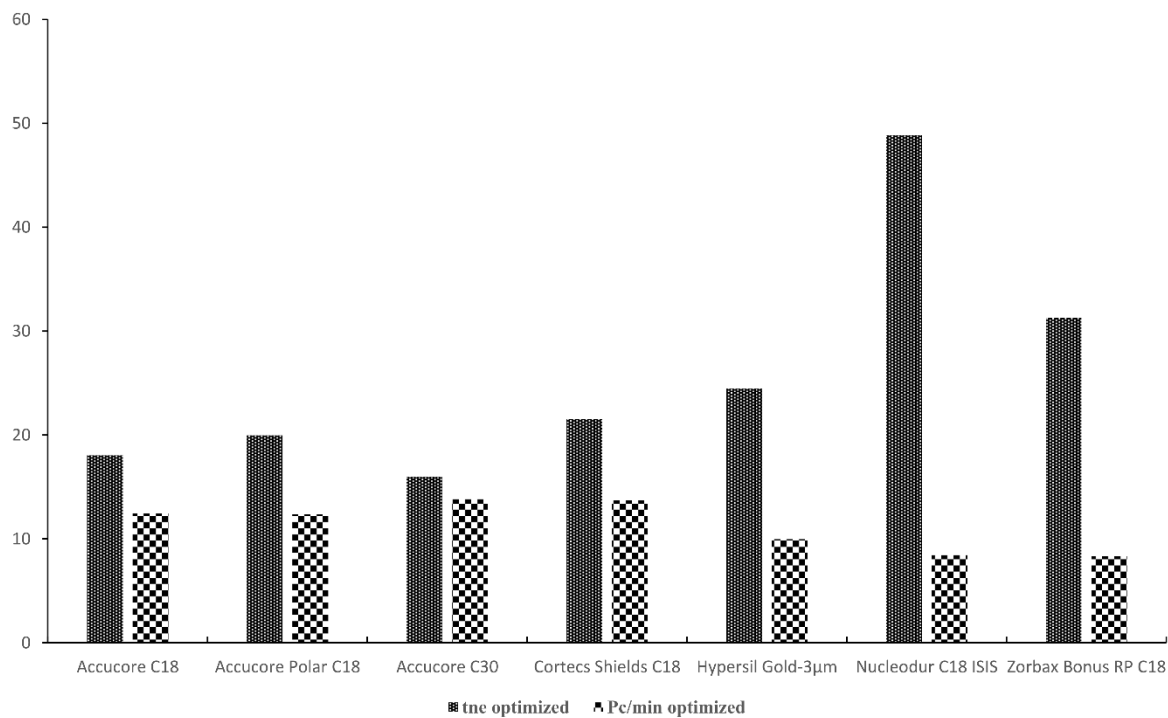
453 According to theoretical calculation of time needed, Accucore C30 emerged as the fastest  
 454 (15 min) for eicosanoids separation followed by Accucore C18 (18min). Zorbax Bonus-RP  
 455 and Nucleodur Isis C18 stood out with a long-time analysis in optimized gradient  
 456 (respectively 31 and 48 min: Fig.7).

457 Experimental results accorded with calculations. Results revealed that Accucore C30  
 458 separated all eicosanoids and PUFA in 6.7 minutes and the longest analysis took 9.8 minutes  
 459 for Nucleodur C18. Accucore C30 was the fastest and the most selective column. Even if  
 460 Accucore C30 and Cortecs Shield C18 had comparable peak capacity per minute in optimized  
 461 gradient (Fig.8), Accucore C30 remained the best because of the minimal  $t_{ne}$  among all  
 462 columns.



463

464 **Fig.7: Evaluation of time needed for eicosanoids mixture separation within seven stationary phases.** Linear gradient  
 465 (Mobile phase: A (water:ACN, 70:30,v/v) containing 0.04% HCOOH; B(Acetonitrile,100,v) containing 0.04%HCOOH ; T =  
 466 25°C ; V injec = 1µL ; Flow rate = 0.5mL/min). For optimized gradient, see **Electronic Supplementary Material, ESM\_2**  
 467 **table 2 and table 3.**



468

469 **Fig.8: Summary of tne and peak capacity per minute for all stationary phases in optimized gradient.** For Optimized  
 470 gradient and chromatographic conditions, see **Electronic Supplementary Material, ESM\_2 table 2 and table 3.**



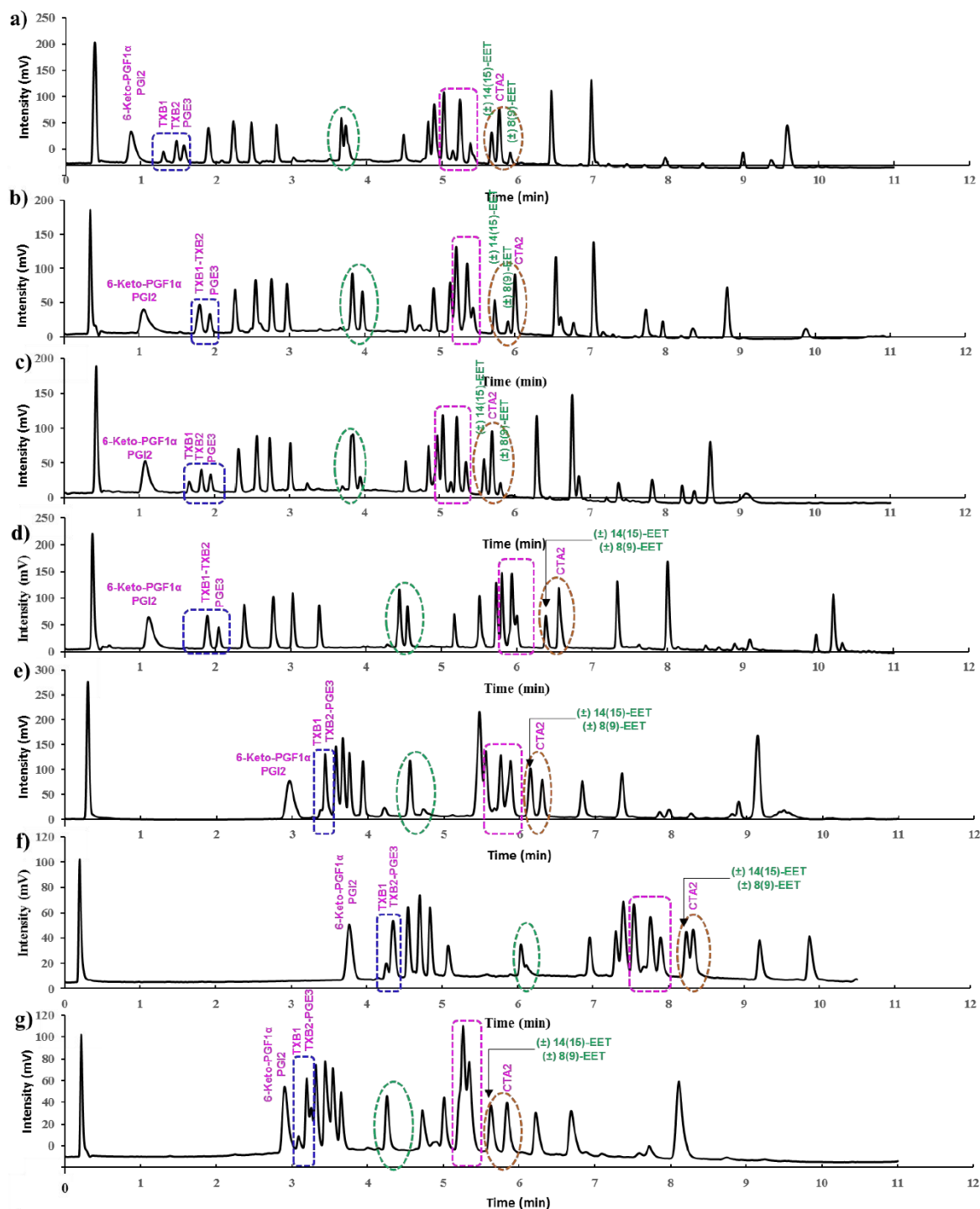
## 471 **4.6 Investigation of columns' dependent chromatographic profiles**

472 Analysis of chromatographic profiles – obtained in optimized gradient for each column –  
473 underlines differences in selectivity. Classical columns (Fig.9.e, f, g) separated prostanoids  
474 with a resolution close to 1 and showed a co-elution of oxidized derivatives such as HETE  
475 and HODE. Eicosanoids profiling took between 8 to 10 minutes. For all fully porous particles  
476 column (Fig.9.e, f and g), several co-elutions emerged: thromboxanes (surrounded in dotted  
477 blue color), HETEs (encircled in dotted pink) , and EETs (encircled in dotted brown).  
478 Superficially porous particles stationary phases except Cortecs Shield C18 offered a profiling  
479 of 7 minutes and presented satisfactory selectivity for PGs and HETEs. We also noted some  
480 differences in elution: superficially porous particles EPG columns are unable to discriminate  
481 thromboxanes (TXB1 and TXB2) and epoxy-eicosatetraenoic acid ((±)14(15)-EET and  
482 (±)8(9)-EET). Conferring to the terms A, B, C of the hydrophobic subtraction model, co-  
483 elution observed for EPG columns could be due to secondary polar interactions between the  
484 EPG (and / or silanols) and eicosanoids.

485 In a target study of eicosanoids in the context of atherosclerosis conducted on 18 eicosanoids  
486 and comparing various column chemistries (C8, C18, PFP, Polar-RP), Rago, *et al.*[18]  
487 selected Synergi Fusion-RP column which offered the best overall selectivity and resolution  
488 for the panel of compounds. Synergi Fusion-RP column is a C18 column with ether linked  
489 phenyl as EPG which mediates secondary polar interactions with polar groups of oxylipins  
490 [18]. Our study conducted on 24 eicosanoids illustrated a better selectivity compared to [18]  
491 between 14,15-EET and 8,9-EET, 15-HETE and 8-HETE (subsection 4.7.2).

492 We calculated  $F_s$  value for Synergi Fusion-RP column. With a value of 2.74, this stationary  
493 phase presented a predicted selectivity equivalent to Hypersil Gold C18 and Nucleodur Isis  
494 C18.

495 Berkecz and co-workers conducted a comparative study for profiling 64 oxylipins with BEH  
496 C18 column to evaluate the potential of both Ultra High Performance Liquid Chromatography  
497 (UHPLC) and Ultra High Performance Supercritic Fluid Chromatography (UHPSFC) [14].  
498 Overall, the evaluation of isobaric and isomeric species selectivity by UHPSFC and UHPLC  
499 coupled to MS, revealed a better sensitivity for UHPLC [14]. However, some co-elutions  
500 persisted and some species recorded a lesser selectivity with BEH C18 column.



501 **Fig.9: Chromatograms obtained in optimized gradient for each stationary phases.** a) Accucore C18; b) Accucore Polar  
 502 Premium c) Accucore C30; d) Cortecs Shield C18; e) Hypersil Gold C18-3 $\mu$ m; f) Nucleodur Isis C18; g) Zorbax Bonus RP.  
 503 For mobile phases composition as well as details optimized gradients, refer to **Electronic Supplementary Material,**  
 504 **ESM\_2, table 2.** T = 25 ° C; V injected = 1 $\mu$ L; flow rate = 0.5mL/min.

505 Based on our results, Accucore C30 enabled to overcome these co-elutions. For example,  
 506 14,15-DiHETE and 5,6-DiHETE are separated with an appropriate selectivity (subsection  
 507 4.7.2), but are co-eluted according to Berkecz, *et al.* study. Similar selectivity between the

508 HETEs isomers can be pointed out between Accucore C30 profile registered in 6 minutes  
509 (subsection 4.7.2) and Berkecz, *et al.* UHPLC profile acquired in 12 minutes.

510 As expected, the trifunctionally bonded BEH particles of the C18 column gets closer –  
511 according to calculated  $F_s$  parameter – to non-EPG columns (Accucore C30, Accucore C18,  
512 HypersilGold C18 and Nucleodur Isis C18) than columns incorporating a polar group in their  
513 grafting (Accucore Polar Premium, Cortecs Shield RP18 and Zorbax Fusion RP).

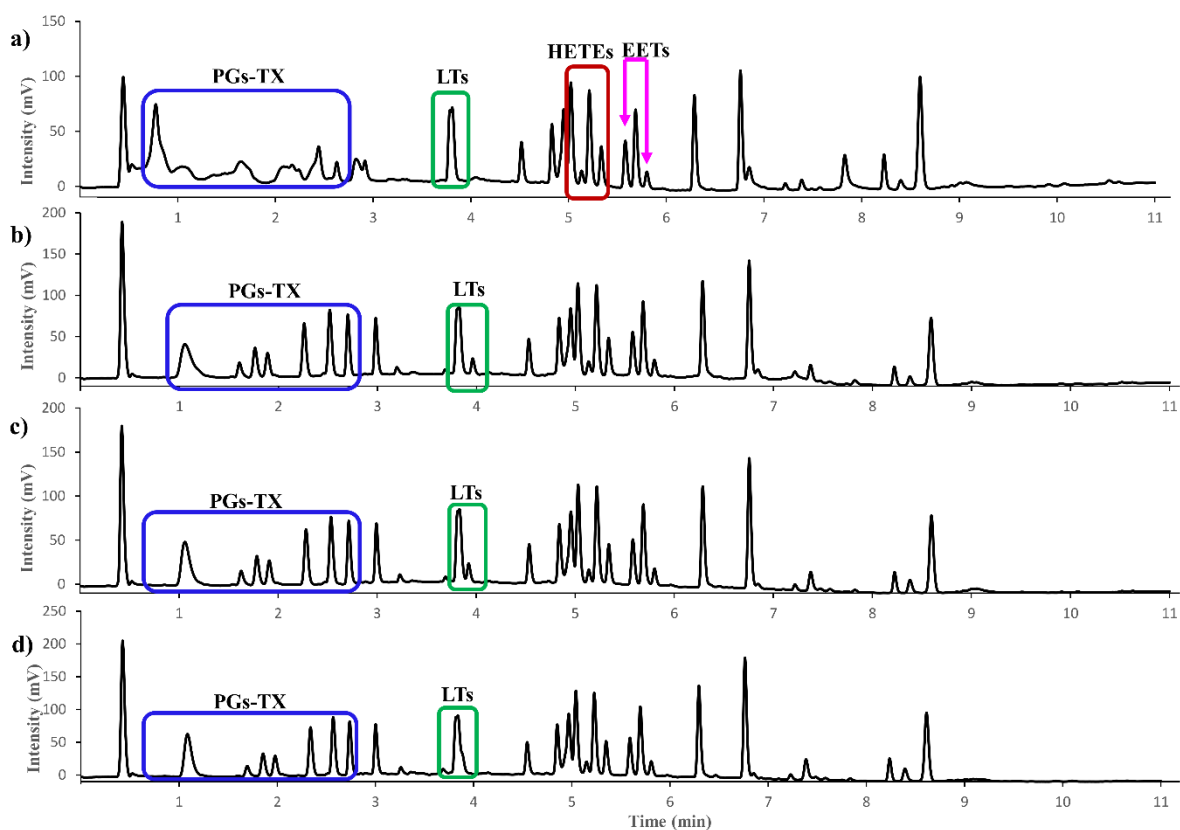
514 Based on the chemistry of Accucore C30 which presented the best selectivity in our study and  
515 results from Acquity UPLC BEH C18 [14] and Synergi Fusion-RP [18] columns, we can  
516 deduce that the use of EPG stationary phases is not determinant to resolve the separation of  
517 eicosanoids with closely related structures. In our study, Accucore C30 – even being the least  
518 retentive – displayed the best selectivity, efficiency and the shortest time for atherosclerosis  
519 related eicosanoids analysis.

## 520 **4.7 The influence of pH and temperature on eicosanoids separation**

521 Regarding our above mentioned results, we only considered the Accucore C30 to determine  
522 the optimal values of pH and temperature.

### 523 **4.7.1 The impact of pH on eicosanoids separation**

524 Different percentages of formic acid (0%, 0.02%, 0.04%, 0.06% and 0.08%) in the mobile  
525 phase are tested. As shown in Fig.10.a (blue), the formic acid seems essential for prostanoids  
526 elution. According to literature, hydroxyeicosatetraenoic acid (HETEs) and oxidized products  
527 are eluted independently of the mobile phase pH but some leukotrienes elution varies with pH  
528 [44, 45]. Leukotrienes elution (Fig.10) confirmed pH impact and is in accordance with  
529 Powell, *et al.* observations [17]. Leukotrienes co-eluted beyond 0.08 % HCOOH (Fig.10.d).  
530 Indeed, peptido-leukotriene such as LTC<sub>4</sub>, LTE<sub>4</sub>, LTF<sub>4</sub> and especially LTD<sub>4</sub> have their  
531 amino group protonated and then induce additional interactions anion exchange with silanols  
532 in acid pH. According to Mathews, *et al.*, the most hydrophobic eicosanoids such as HETEs /  
533 EETs require only a high proportion of organic solvent to ensure good resolution and  
534 efficiency [45]. Based on our results, we considered a pH of 3 – corresponding to 0.04%  
535 formic acid – for eicosanoids analysis.



536

537 **Fig.10: Influence of pH on eicosanoids separation through Accucore C30.** Mobile phase: A (Water:ACN, 70:30,v/v), B  
 538 (Acetonitrile,100,v) containing each a) 0% HCOOH; b) 0.02% HCOOH; c) 0.04% HCOOH; d) 0.08% HCOOH; at T =  
 539 25°C; with a V injec = 1µL; and a flow rate of 0.5 mL/min. PGs-TX: Prostaglandins-Thromboxanes; LT: Leukotrienes.

#### 540 4.7.2 The influence of temperature on eicosanoids separations

541 Temperature increase was not enough to discriminate 6-keto PGF1 $\alpha$  and PGI2 regardless the  
 542 stationary phase in this study (Fig.11-orange). In contrast, an increase in temperature  
 543 improved the asymmetry and tailing factor of this peak. This co-elution relates more to the  
 544 secondary polar interactions: the tailing peak of 6-keto PGF1 $\alpha$  and PGI2 results from a  
 545 hydrogen bonding interaction between a donor hydrogen (from silanols) and the ketone or  
 546 oxygen of hydroxyle group (from 6-keto PGF1 $\alpha$  and PGI2). In addition, it is important to note  
 547 that PGI2 is an unstable cyclooxygenase metabolite at neutral or acid pH which hydrolyzes  
 548 rapidly to 6-keto PGF1 $\alpha$  when exposed to air. Resolution between TXB2 and PGE3 decreased  
 549 beyond 30°C (Fig.11-blue) and co-eluted at 45 °C. During the development, it was very  
 550 difficult to perform the separation of TXB1-TXB2-PGE3 and LTB4-14,15-DiHETE-5,6-  
 551 DiHETE. Fig.12 displays how selectivity varies between some isomers such as TXB1 and  
 552 TXB2 on one hand; and 5,6-DiHETE and 14,15-DiHETE on the other hand. Concerning  
 553 TXB1, TXB2 and PGE3, the selectivity between TXB2 and PGE3 decreased while increasing  
 554 temperature gradually. This observation confirms the steric selectivity which permits to  
 555 discriminate TXB1, TXB2 and PGE3. Considering LTB4 and 14,15-DiHETE, selectivity

556 increased from 20°C (fig.12). In sum, temperature influences the steric recognition for some  
 557 molecules and should be set in function. As the selectivity improvement between isomers was  
 558 one goal in our study as well as profiling 24 eicosanoids, we selected the temperature of 20°C  
 559 as a compromise for eicosanoids separation.

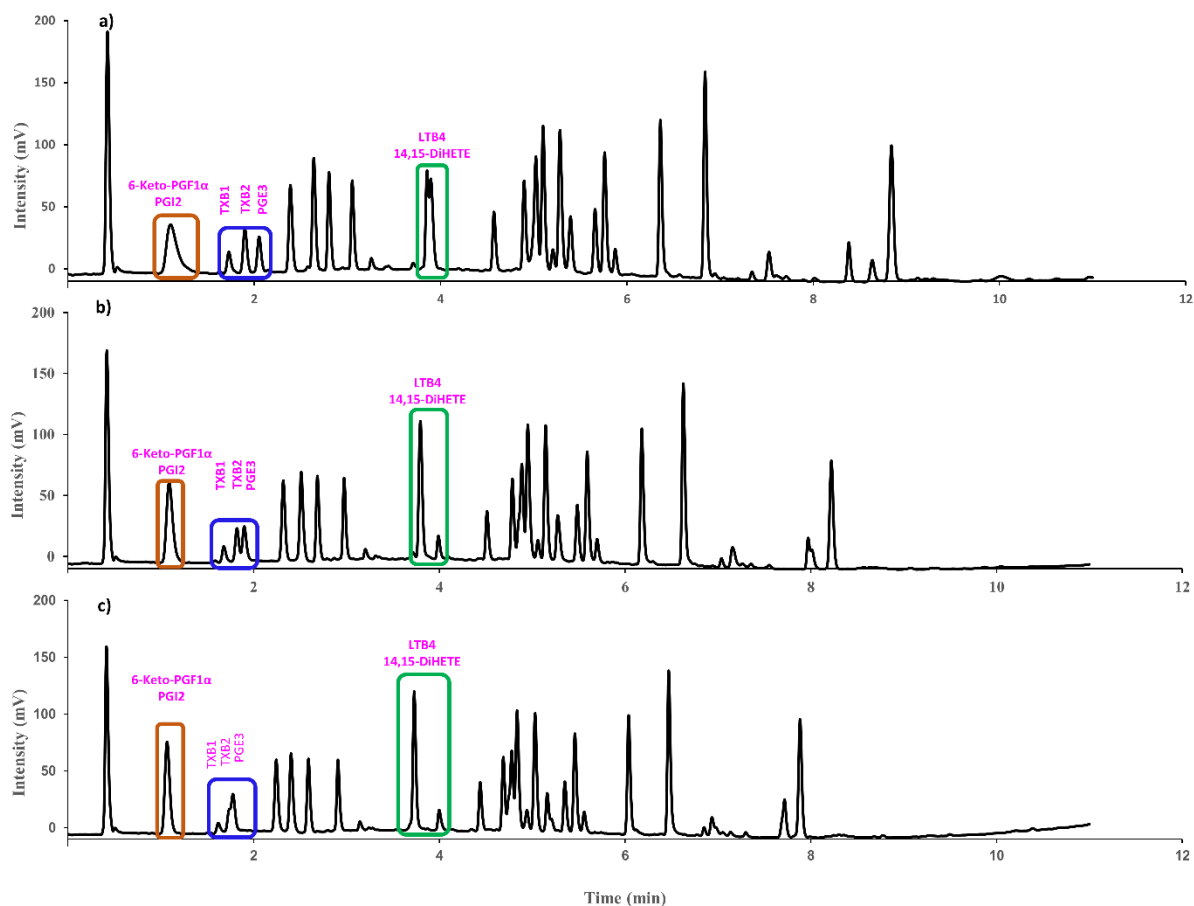
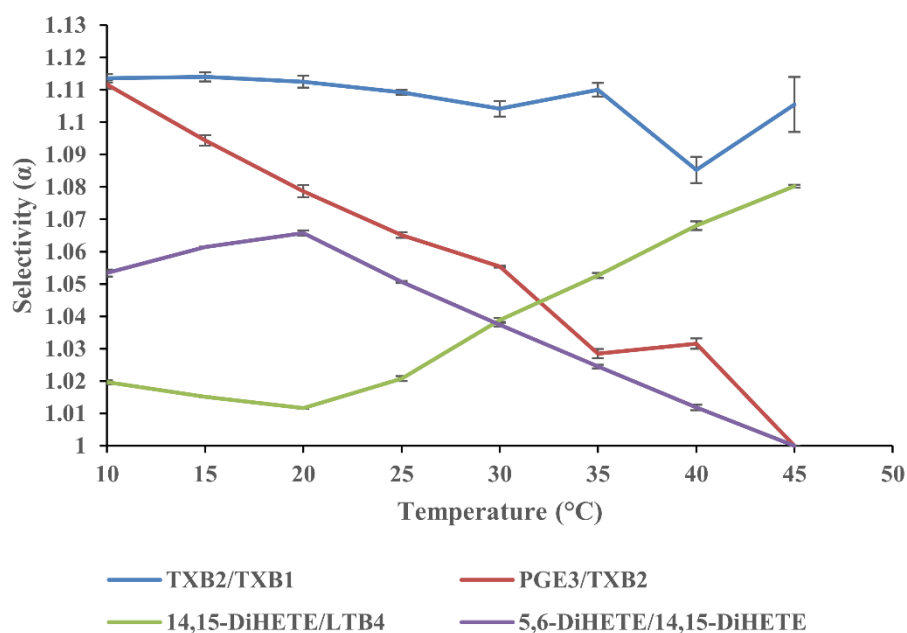
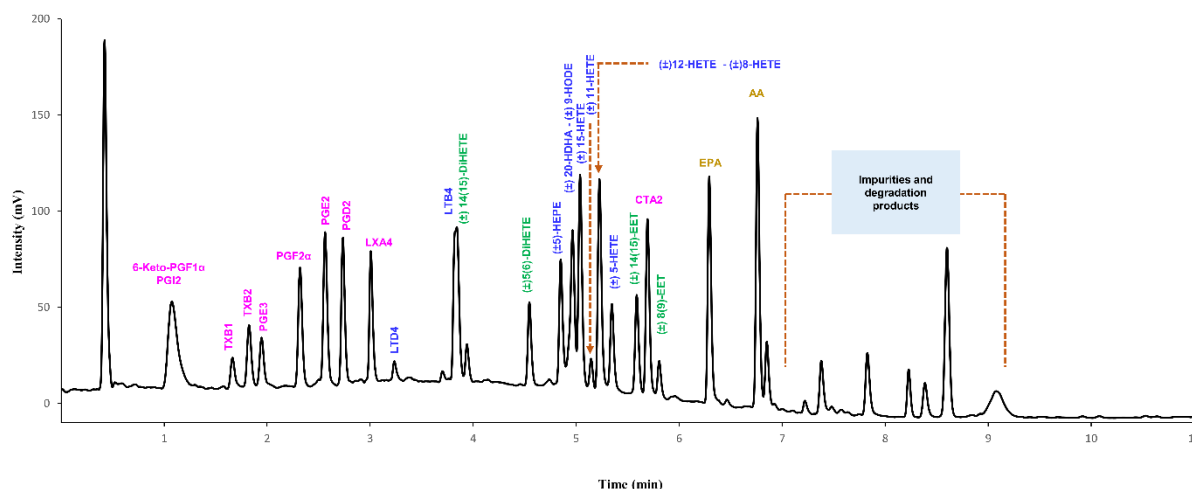


**Fig.11: Influence of temperature on eicosanoids retention.** Stationary phase : Accucore C30 (100mm x 2.1mm x 2.6µm) ; Mobile phase: A (water:ACN, 70:30,v/v) containing 0.04% HCOOH; B(Acetonitrile,100,v) containing 0.04%HCOOH ; a) T = 20°C ; b) T=35°C ; c) T= 45°C ; V injec = 1µL ; Flow rate = 0.5 mL/min.



560 **Fig. 12: Influence of temperature on selectivity between some isomers of eicosanoids during RP-HPLC profiling.**  
 561 Separation was performed from the 26 molecular species of eicosanoids and PUFA in triplicate for each temperature (10°C,  
 562 15°C, 20°C, 25°C, 30°C, 35°C, 40°C and 45°C), average and standard deviation are presented for each temperature.  
 563 Stationary phase: Accucore C30 (100mm x 2.1mm x 2.6µm); Mobile phase: A (water:ACN, 70:30,v/v) containing 0.04%  
 564 HCOOH; B(Acetonitrile,100,v) containing 0.04%HCOOH; V injec = 1µL ; Flow rate = 0.5 mL/min.

Regardless of the optimization conditions (mobile phase composition, temperature, pH), the first peak of the chromatogram corresponded to a co-elution of 6-Keto PGF1α and PGI2. Fig.13 displays the best chromatographic profile of 26 molecular species on Accucore C30 at pH=3 and T=20°C. Accucore C30 displayed the best selectivity, efficiency and procured the fastest acquisition time among the seven-screened columns. The most polar eicosanoids such as prostaglandins and thromboxanes eluted early with a good selectivity. Leukotrienes and related oxidized eicosanoids eluted towards the end of the gradient with a higher proportion of organic phase.



565 **Fig.13: Profiling of 24 eicosanoids and 2 polyunsaturated fatty acids by reverse phase ultra-high performance liquid**  
 566 **chromatography coupled to corona-CAD® detector.** Stationary phase: Accucore C30 (100 x 2.1 mm x 2.6µm); Mobile

567 phase: A (water: acetonitrile, 70:30, v/v); B (Acetonitrile, 100, v) containing 0.04% HCOOH each, at 20°C with V injec =  
568 1 µL and a flow rate of 0.5 mL/min.

## 569 **5 Conclusion:**

570 Eicosanoids occur at traces level in biological samples and present many isomers and isobars.  
571 Therefore, chromatographic performances in terms of selectivity should be improved to  
572 resolve co-elutions and to permit their quantification in complex matrices (i.e.: cellular  
573 matrices). Various column selection systems have been reported for chromatographic  
574 characterization of stationary phases. It is difficult to decide on the procedure to select an  
575 appropriate column especially when analyzing close structure molecules such as eicosanoids.  
576 In the present study, hydrophobic subtraction model helped us to select columns with  
577 different predicted selectivity. In this context, the complementary between  $F_s$  parameter and  
578 radar plots for columns performance discrimination was highlighted. Chromatographic  
579 performance descriptors guided us to select the suitable stationary phase for atherosclerosis  
580 related eicosanoids analysis. Analysis on Accucore C30 – the least retentive column with a  $t_{ne}$   
581 of 15 minutes – lasted around 7 minutes. Accucore C30 displayed the best selectivity,  
582 efficiency and the shorter time for eicosanoids analysis, even being the least retentive. The  
583 present study demonstrated the interest of using Accucore columns for lipid analysis – herein  
584 the different subfamilies of eicosanoids.

585 Reverse phase liquid chromatography has been previously reported as an appropriate method  
586 for eicosanoids analysis even though the separation of regioisomers remained an unresolved  
587 issue [2, 18, 27]. Anticipating new developments in core-shell and/or sub-2µm stationary  
588 phases chemistry as well as the possibilities offered by SFC in addition to HPLC, significant  
589 improvements in structurally close molecules separation can be expected. For example, using  
590 a 2-PIC stationary phase, Ubhayasekera, et al. [13], published a rapid SFC-MS method able to  
591 quantify 4 prostanoids and 1 leukotriene with a run time of 3 minutes and a satisfactory,  
592 selectivity. However, our study confirmed the difficulty of separating eicosanoids isomers  
593 involved in physiopathological process. In addition, it demonstrated the imperative need to  
594 select RP-HPLC stationary phases with different selectivity. This approach is particularly  
595 appropriate because it allows rapid selection of the appropriate column and permits to reach  
596 the desired selectivity for particular molecules such as eicosanoids. The present study  
597 demonstrated the interest of using Accucore columns for lipid analysis – herein the different  
598 sub-families of eicosanoids.

599 **6 Acknowledgements**

600 This work took place thanks to a funding by a PhD scholarship from the French Ministry of  
601 Higher Education, Research and Innovation (MESRI). The authors also thank the  
602 representatives of Thermo Fisher Scientific and Waters for the gracious loan of their columns.  
603

604 **7 Conflict of interest**

605 The authors declare that they have no conflict of interest.



## 606 8 References

607

608 1. Chhonker YS, Bala V, Murry DJ (2018) Quantification of eicosanoids and their  
609 metabolites in biological matrices: a review. *Bioanalysis* 10:2027–2046 .  
610 <https://doi.org/10.4155/bio-2018-0173>

611 2. Kortz L, Dorow J, Becker S, Thiery J, Ceglarek U (2013) Fast liquid chromatography–  
612 quadrupole linear ion trap-mass spectrometry analysis of polyunsaturated fatty acids and  
613 eicosanoids in human plasma. *Journal of Chromatography B* 927:209–213 .  
614 <https://doi.org/10.1016/j.jchromb.2013.03.012>

615 3. Astarita G, Kendall AC, Dennis EA, Nicolaou A (2015) Targeted lipidomic strategies  
616 for oxygenated metabolites of polyunsaturated fatty acids. *Biochimica et Biophysica*  
617 *Acta (BBA) - Molecular and Cell Biology of Lipids* 1851:456–468 .  
618 <https://doi.org/10.1016/j.bbalip.2014.11.012>

619 4. Tsikas D, Zoerner AA (2014) Analysis of eicosanoids by LC-MS/MS and GC-MS/MS:  
620 A historical retrospect and a discussion. *Journal of Chromatography B* 964:79–88 .  
621 <https://doi.org/10.1016/j.jchromb.2014.03.017>

622 5. Peres-Buzalaf C, de Paula L, Frantz FG, Soares EM, Medeiros AI, Peters-Golden M,  
623 Silva CL, Faccioli LH (2011) Control of experimental pulmonary tuberculosis depends  
624 more on immunostimulatory leukotrienes than on the absence of immunosuppressive  
625 prostaglandins. *Prostaglandins, Leukotrienes and Essential Fatty Acids* 85:75–81 .  
626 <https://doi.org/10.1016/j.plefa.2011.04.024>

627 6. Dumlao DS, Buczynski MW, Norris PC, Harkewicz R, Dennis EA (2011) High-  
628 throughput lipidomic analysis of fatty acid derived eicosanoids and N-  
629 acylethanolamines. *Biochimica et Biophysica Acta (BBA) - Molecular and Cell Biology*  
630 *of Lipids* 1811:724–736 . <https://doi.org/10.1016/j.bbalip.2011.06.005>

631 7. Galvão AF, Petta T, Flamand N, Bollela VR, Silva CL, Jarduli LR, Malmegrim KCR,  
632 Simões BP, de Moraes LAB, Faccioli LH (2016) Plasma eicosanoid profiles determined  
633 by high-performance liquid chromatography coupled with tandem mass spectrometry in  
634 stimulated peripheral blood from healthy individuals and sickle cell anemia patients in  
635 treatment. *Anal Bioanal Chem* 408:3613–3623 . <https://doi.org/10.1007/s00216-016-9445-8>  
636

637 8. Martin-Venegas R, Jáuregui O, Moreno JJ (2014) Liquid chromatography-tandem mass  
638 spectrometry analysis of eicosanoids and related compounds in cell models. *Journal of*  
639 *Chromatography B* 964:41–49 . <https://doi.org/10.1016/j.jchromb.2014.05.024>

640 9. VanRollins M, VanderNoot VA (2003) Simultaneous resolution of underivatized  
641 regioisomers and stereoisomers of arachidonate epoxides by capillary electrophoresis.  
642 *Analytical Biochemistry* 11

643 10. Buczynski MW, Stephens DL, Bowers-Gentry RC, Grkovich A, Deems RA, Dennis EA  
644 (2007) TLR-4 and Sustained Calcium Agonists Synergistically Produce Eicosanoids  
645 Independent of Protein Synthesis in RAW264.7 Cells. *J Biol Chem* 282:22834–22847 .  
646 <https://doi.org/10.1074/jbc.M701831200>

- 647 11. Ferreiro-Vera C, Mata-Granados JM, Priego-Capote F, Luque de Castro MD (2011)  
648 Automated method for targeting analysis of prostanoids in human serum by on-line  
649 solid-phase extraction and liquid chromatography–mass spectrometry in selected  
650 reaction monitoring. *Journal of Chromatography A* 1218:2848–2855 .  
651 <https://doi.org/10.1016/j.chroma.2011.03.049>
- 652 12. Dufлот T, Pereira T, Roche C, Iacob M, Cardinael P, Hamza NE-G, Thuillez C,  
653 Compagnon P, Joannidès R, Lamoureux F, Bellien J (2016) A sensitive LC-MS/MS  
654 method for the quantification of regioisomers of epoxyeicosatrienoic and  
655 dihydroxyeicosatrienoic acids in human plasma during endothelial stimulation.  
656 *Analytical and Bioanalytical Chemistry* 409:1845–1855 .  
657 <https://doi.org/10.1007/s00216-016-0129-1>
- 658 13. Ubhayasekera SJKA, R. Acharya S, Bergquist J (2018) A novel, fast and sensitive  
659 supercritical fluid chromatography-tandem mass spectrometry (SFC-MS/MS) method  
660 for analysis of arachidonic acid metabolites. *Analyst* 143:3661–3669 .  
661 <https://doi.org/10.1039/C8AN00788H>
- 662 14. Berkecz R, Lísa M, Holčapek M (2017) Analysis of oxylipins in human plasma:  
663 Comparison of ultrahigh-performance liquid chromatography and ultrahigh-performance  
664 supercritical fluid chromatography coupled to mass spectrometry. *Journal of*  
665 *Chromatography A* 1511:107–121 . <https://doi.org/10.1016/j.chroma.2017.06.070>
- 666 15. Kohno S, Keenan AL, Ntambi JM, Miyazaki M (2018) Lipidomic insight into  
667 cardiovascular diseases. *Biochemical and Biophysical Research Communications*  
668 504:590–595 . <https://doi.org/10.1016/j.bbrc.2018.04.106>
- 669 16. Aghazadeh-Habashi A, Asghar W, Jamali F (2015) Simultaneous determination of  
670 selected eicosanoids by reversed-phase HPLC method using fluorescence detection and  
671 application to rat and human plasma, and rat heart and kidney samples. *Journal of*  
672 *Pharmaceutical and Biomedical Analysis* 110:12–19 .  
673 <https://doi.org/10.1016/j.jpba.2015.02.041>
- 674 17. Powell WS (1985) High Pressure Liquid Chromatography of Eicosanoids. In: Lands  
675 WEM (ed) *Biochemistry of Arachidonic Acid Metabolism*. Springer US, Boston, MA,  
676 pp 375–403
- 677 18. Rago B, Fu C (2013) Development of a high-throughput ultra performance liquid  
678 chromatography–mass spectrometry assay to profile 18 eicosanoids as exploratory  
679 biomarkers for atherosclerotic diseases. *Journal of Chromatography B* 936:25–32 .  
680 <https://doi.org/10.1016/j.jchromb.2013.08.001>
- 681 19. Žuvela P, Skoczylas M, Jay Liu J, Bączek T, Kaliszan R, Wong MW, Buszewski B  
682 (2019) Column Characterization and Selection Systems in Reversed-Phase High-  
683 Performance Liquid Chromatography. *Chem Rev* 119:3674–3729 .  
684 <https://doi.org/10.1021/acs.chemrev.8b00246>
- 685 20. Horváth C, Melander W, Molnár I (1976) Solvophobic interactions in liquid  
686 chromatography with nonpolar stationary phases. *Journal of Chromatography A*  
687 125:129–156 . [https://doi.org/10.1016/S0021-9673\(00\)93816-0](https://doi.org/10.1016/S0021-9673(00)93816-0)

- 688 21. Snyder L, Dolan J, Carr P (2004) The hydrophobic-subtraction model of reversed-phase  
689 column selectivity. *Journal of Chromatography A* 1060:77–116 .  
690 [https://doi.org/10.1016/S0021-9673\(04\)01480-3](https://doi.org/10.1016/S0021-9673(04)01480-3)
- 691 22. HPLC Columns - HPLC column selectivity measurements of more than 600 reversed  
692 phase columns from over 30 manufacturers. <http://www.hplccolumns.org/index.php>.  
693 Accessed 24 Sep 2019
- 694 23. Horvath CG, Lipsky SR (1967) Peak capacity in chromatography. *Anal Chem* 39:1893–  
695 1893 . <https://doi.org/10.1021/ac50157a075>
- 696 24. Neue UD (2005) Theory of peak capacity in gradient elution. *Journal of*  
697 *Chromatography A* 1079:153–161 . <https://doi.org/10.1016/j.chroma.2005.03.008>
- 698 25. Schoenmakers PJ (1986) *Optimization of Chromatographic Selectivity: A Guide to*  
699 *Method Development*. Elsevier
- 700 26. Kortz L, Dorow J, Ceglarek U (2014) Liquid chromatography–tandem mass  
701 spectrometry for the analysis of eicosanoids and related lipids in human biological  
702 matrices: A review. *Journal of Chromatography B* 964:1–11 .  
703 <https://doi.org/10.1016/j.jchromb.2014.01.046>
- 704 27. Deems R, Buczynski MW, Bowers- Gentry R, Harkewicz R, Dennis EA (2007)  
705 Detection and Quantitation of Eicosanoids via High Performance Liquid  
706 Chromatography- Electrospray Ionization- Mass Spectrometry. In: *Methods in*  
707 *Enzymology*. Academic Press, pp 59–82
- 708 28. Moncada S (1983) Biology and therapeutic potential of prostacyclin. *Stroke* 14:157–168  
709 . <https://doi.org/10.1161/01.str.14.2.157>
- 710 29. Gilroy JJ, Dolan JW, Snyder LR (2003) Column selectivity in reversed-phase liquid  
711 chromatography: IV. Type-B alkyl-silica columns. *Journal of Chromatography A*  
712 1000:757–778 . [https://doi.org/10.1016/S0021-9673\(03\)00512-0](https://doi.org/10.1016/S0021-9673(03)00512-0)
- 713 30. Wilson NS, Gilroy J, Dolan JW, Snyder LR (2004) Column selectivity in reversed-phase  
714 liquid chromatography: VI. Columns with embedded or end-capping polar groups.  
715 *Journal of Chromatography A* 1026:91–100 .  
716 <https://doi.org/10.1016/j.chroma.2003.11.041>
- 717 31. Žuvela P, Skoczylas M, Jay Liu J, Bączek T, Kaliszan R, Wong MW, Buszewski B  
718 (2019) Column Characterization and Selection Systems in Reversed-Phase High-  
719 Performance Liquid Chromatography. *Chem Rev* 119:3674–3729 .  
720 <https://doi.org/10.1021/acs.chemrev.8b00246>
- 721 32. Tamba Sompila AWG, Héron S, Hmida D, Tchaplal A (2017) Fast non-aqueous  
722 reversed-phase liquid chromatography separation of triacylglycerol regioisomers with  
723 isocratic mobile phase. Application to different oils and fats. *Journal of Chromatography*  
724 *B* 1041–1042:151–157 . <https://doi.org/10.1016/j.jchromb.2016.12.030>
- 725 33. Tanaka N, McCalley DV (2016) Core–Shell, Ultrasmall Particles, Monoliths, and Other  
726 Support Materials in High-Performance Liquid Chromatography. *Anal Chem* 88:279–  
727 298 . <https://doi.org/10.1021/acs.analchem.5b04093>

- 728 34. Gritti F, Guiochon G (2010) Mass transfer resistance in narrow-bore columns packed  
729 with 1.7 $\mu$ m particles in very high pressure liquid chromatography. *Journal of*  
730 *Chromatography A* 1217:5069–5083 . <https://doi.org/10.1016/j.chroma.2010.05.059>
- 731 35. Gritti F, Shiner SJ, Fairchild JN, Guiochon G (2014) Evaluation of the kinetic  
732 performance of new prototype 2.1mm $\times$ 100mm narrow-bore columns packed with 1.6 $\mu$ m  
733 superficially porous particles. *Journal of Chromatography A* 1334:30–43 .  
734 <https://doi.org/10.1016/j.chroma.2014.01.065>
- 735 36. Bruns S, Stoeckel D, Smarsly BM, Tallarek U (2012) Influence of particle properties on  
736 the wall region in packed capillaries. *Journal of Chromatography A* 1268:53–63 .  
737 <https://doi.org/10.1016/j.chroma.2012.10.027>
- 738 37. Gritti F, Guiochon G (2014) The rationale for the optimum efficiency of columns packed  
739 with new 1.9 $\mu$ m fully porous Titan-C18 particles—A detailed investigation of the intra-  
740 particle diffusivity. *Journal of Chromatography A* 1355:164–178 .  
741 <https://doi.org/10.1016/j.chroma.2014.05.076>
- 742 38. Gritti F, Guiochon G (2010) Mass transfer mechanism in liquid chromatography  
743 columns packed with shell particles: Would there be an optimum shell structure? *Journal*  
744 *of Chromatography A* 1217:8167–8180 . <https://doi.org/10.1016/j.chroma.2010.10.075>
- 745 39. Martin M, Thevenon G, Tchaplal A (1988) Comparison of retention mechanisms of  
746 homologous series and triglycerides in non-aqueous reversed-phase liquid  
747 chromatography. *Journal of Chromatography A* 452:157–173 .  
748 [https://doi.org/10.1016/S0021-9673\(01\)81445-X](https://doi.org/10.1016/S0021-9673(01)81445-X)
- 749 40. Tchaplal Alain, Colin Henri, Guiochon Georges (1984) Linearity of homologous series  
750 retention plots in reversed-phase liquid chromatography. *Anal Chem* 56:621–625 .  
751 <https://doi.org/10.1021/ac00268a007>
- 752 41. Dorset DL, Pangborn WA, Hancock AJ, van Soest TC, Greenwald SM (1978) Glycerol  
753 Conformation and the Crystal Structure of Lipids II. A Further Study of Tripalmitin and  
754 Conformationally Fixed Analogs by Small-Angle X-Ray Diffraction and Reflection  
755 Electron Diffraction. *Zeitschrift für Naturforschung C* 33:50–55 .  
756 <https://doi.org/10.1515/znc-1978-1-209>
- 757 42. Neue UD, Cheng Y-F, Lu Z, Alden BA, Iraneta PC, Khoebe CH, Van Tran K (2001)  
758 Properties of reversed phase packings with an embedded polar group. *Chromatographia*  
759 54:169–177 . <https://doi.org/10.1007/BF02492239>
- 760 43. Kirkland JJ, Henderson JW, Martosella JD, Bidlingmeyer BA, Vasta-Russel J, Adams Jr  
761 JB (1999) A Highly Stable Alkyl–Amide Silica-Based Column Packing for Silica-Based  
762 Column Packing for Reversed-Phase HPLC of Polar Reversed-Phase HPLC of Polar and  
763 Ionizable Compounds and Ionizable Compound. *LCGC North América* 17:634
- 764 44. Powell WS (1985) Reversed-phase high-pressure liquid chromatography of arachidonic  
765 acid metabolites formed by cyclooxygenase and lipoxygenases. *Analytical Biochemistry*  
766 148:59–69 . [https://doi.org/10.1016/0003-2697\(85\)90628-1](https://doi.org/10.1016/0003-2697(85)90628-1)

767 45. Mathews WR, Rokach J, Murphy RC (1981) Analysis of leukotrienes by high-pressure  
768 liquid chromatography. *Analytical Biochemistry* 118:96–101 .  
769 [https://doi.org/10.1016/0003-2697\(81\)90162-7](https://doi.org/10.1016/0003-2697(81)90162-7)

770